Appendix A

Expressions of the Eshelby's tensor

Analytical formulae of the Eshelby's tensor were introduced by Eshelby [30] for isotropic materials and spheroids. Later, Withers [108] extended the expressions to transversely isotropic medium, with the restriction that the direction of anisotropy has the same orientation as the aligned reinforcements. In all other cases (ellipsoidal inclusions and/or anisotropic material), a numerical evaluation of the tensor is necessary and was implemented by Gavazzi and Lagoudas [34].

A.1 Isotropic matrix

Hereafter are given the non-nil components of the Eshelby's tensor for spheroids of aspect ratio Ar embedded in an isotropic matrix (expressions are picked up from Friebel [32]). Reinforcements are aligned along the direction 1.

$$\begin{aligned} S_{1111} &= \frac{1}{2(1-\nu)}\left[2(1-\nu)(1-g)+g-Ar^2\frac{3g-2}{Ar^2-1}\right], \\ S_{2222}=S_{3333} &= \frac{1}{4(1-\nu)}\left[2(2-\nu)g-\frac{1}{2}-(Ar^2-\frac{1}{4})\frac{3g-2}{Ar^2-1}\right], \end{aligned}$$

$$
\begin{aligned}
S_{1122} = S_{1133} &= \frac{1}{4(1-\nu)}\left[4\nu(1-g) - g + Ar^2\frac{3g-2}{Ar^2-1}\right], \\
S_{2233} = S_{3322} &= \frac{1}{4(1-\nu)}\left[-(1-2\nu)g + \frac{1}{2} - \frac{1}{4}\frac{3g-2}{Ar^2-1}\right], \\
S_{2211} = S_{3311} &= \frac{1}{4(1-\nu)}\left[-(1-2\nu)g + Ar^2\frac{3g-2}{Ar^2-1}\right], \\
S_{1212} = S_{1313} &= \frac{1}{4(1-\nu)}\left[(1-\nu)(2-g) - g + Ar^2\frac{3g-2}{Ar^2-1}\right], \\
S_{2323} &= \frac{S_{2222} - S_{1122}}{2}, \qquad \text{(A.1)}
\end{aligned}
$$

where:

$$
\begin{aligned}
g &= \frac{Ar}{(Ar^2-1)^{3/2}}\left[Ar(Ar^2-1)^{1/2} - cos^{-1}Ar\right] \text{ for } 0 < Ar < 1, \\
g &= \frac{Ar}{(1-Ar^2)^{3/2}}\left[cosh^{-1}Ar - Ar(1-Ar^2)^{1/2}\right] \text{ for } 1 < Ar < \infty. \qquad \text{(A.2)}
\end{aligned}
$$

Eshelby's tensor has the minor symmetries ($S_{ijkl} = S_{jikl} = S_{ijlk} = S_{jilk}$) but not the major ones ($S_{ijkl} = S_{klij}$).

For the particular case of spherical inclusions, previous equations become invalid and require a study of these functions around $Ar = 1$. This gives:

$$
\begin{aligned}
S_{1111} = S_{2222} = S_{3333} &= \frac{7-5\nu}{15(1-\nu)}, \\
S_{1122} = S_{1133} = S_{2233} &= \frac{5\nu-1}{15(1-\nu)}, \\
S_{1212} = S_{1313} = S_{2323} &= \frac{4-5\nu}{15(1-\nu)}. \qquad \text{(A.3)}
\end{aligned}
$$

A.2 Transversely isotropic matrix

Eshelby's results are based on the solution of a point force applied inside an infinite solid. Solution of this problem is given by the elastic Green's functions. An explicit solution of the Green's function in a general anisotropic medium is possible only if a sixth-order algebraic equation has six different roots. For transversely isotropic materials this condition is reduced to (direction of anisotropy is 1):

$$
(C_{1111}C_{3333})^{1/2} - C_{1133} - C_{2323} \neq 0. \qquad \text{(A.4)}
$$

Analytical point force solution for an infinite transversely isotropic solid was given by Pan and Chou [76].

Starting from the solution of this problem, Withers [108] developed the expression of Eshelby's tensor for transversely isotropic medium under the condition that the direction of anisotropy is the same as the aligned inclusions. Components of this tensor are function of several constants and two integrals over the volume of the ellipsoid. Developments of Withers remain valid only if expression (A.4) is positive. However, when performing all the computations with complex calculus, one can prove that the integrals in the two cases are complex conjugate and equals. They are thus real as well as the final result of the Eshelby's tensor.

Appendix B

Laplace-Carson transform and its inversion

B.1 Laplace-Carson transform

The Laplace-Carson transform is defined by:

$$[\mathcal{L}(f)]_{(s)} = f^*(s) = s\int_0^\infty f(t)e^{-st}dt. \tag{B.1}$$

It is thus the classical Laplace transform multiplied by the Laplace variable s. Main advantages of this transform are that a constant remains a constant, the time derivative of one of the members in a convolution product disappears under this transform and the transform of a Stieljes type convolution product is reduced to a single contraction between the transform of the two operands. Some basic Laplace-Carson transforms are given in table B.1.

B.2 Laplace-Carson inversion

The collocation method proposed by Scharpery [90] for numerical inversion of the Laplace-Carson transform is adopted. Main advantages of this method are the ease of its implementation, its efficiency and the analytical form of the result so that the time function can be evaluated at any time.

Consider an expression $f^*(s)$ known in the Laplace domain. A development of the unknown time function into a Dirichlet series for a particular choice of basis functions gives:

$$f(t) = A + Bt + \sum_{k=1}^{k=M} b_k \underbrace{\left(1 - e^{-t/\theta_k}\right)}_{\text{Basis functions}}. \tag{B.2}$$

$f(t)$	$f^*(s)$	Conditions
a	a	$s > 0$
at	a/s	$s > 0$
e^{at}	$\frac{s}{s-a}$	$s > a$
$cos(\omega t)$	$\frac{s^2}{s^2+\omega^2}$	-
$\delta(t-c)$	se^{-cs}	-
$H(t-c)$	e^{-cs}	-
$af(t)+bg(t)$	$af^*(s)+bg^*(s)$	-
$A \otimes B$	$\frac{1}{s}A^*(s) : B^*(s)$	-
$A \odot B$	$A^*(s) : B^*(s)$	-

Table B.1: Basic Laplace-Carson transforms.

Main advantage of this decomposition is that its Laplace-Carson transform is known analytically:

$$f^*(s) = A + \frac{B}{s} + \sum_{k=1}^{k=M} b_k \underbrace{\frac{1}{1+s\theta_k}}_{\text{Transf. basis funct.}}, \tag{B.3}$$

where θ_k are given relaxation times chosen equispaced on a logarithmic scale. Bounds and length of this interval can have a considerable impact on the results.

In expression (B.3), A and B are limit values which can be evaluated from the known function in the Laplace or time domain:

$$A = \lim_{s\to+\infty} f^*(s) = \lim_{t\to 0} f(t), \tag{B.4}$$

$$B = \lim_{s\to 0} sf^*(s) = \lim_{t\to+\infty} \frac{f(t)}{t}. \tag{B.5}$$

The only unknowns in expression (B.3) are the factors b_k. In order to calculate them, the function in the Laplace domain is evaluated at M collocation points $s_l = 1/\theta_l$:

$$f^*(s_l) = A + \frac{B}{s_l} + \sum_{k=1}^{k=M} b_k \frac{1}{1+s_l\theta_k}, \qquad 1 \le l \le M. \tag{B.6}$$

Typically, around 20 points are enough. Better precision can be obtained when increasing the number of collocation points but the system then becomes larger and can even get close to singular. For computing the factors b_k, a linear system of size M must be solved. Once the M unknowns b_k are found, the time function (B.2) can be evaluated at any time.

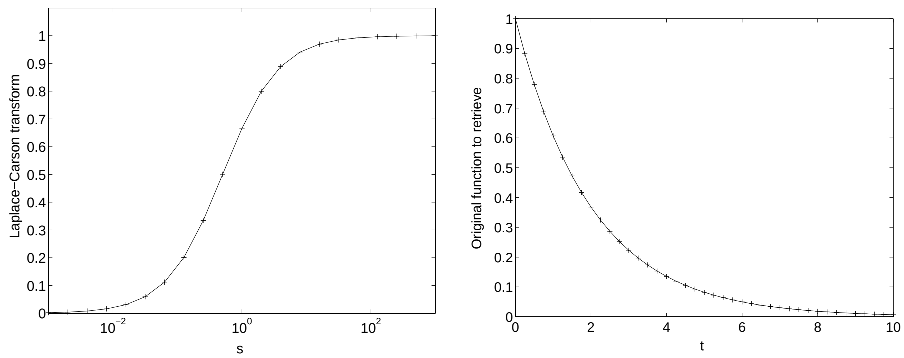

(a) Laplace domain. (b) Time domain.

Figure B.1: Numerical inversion of the transform of a decreasing exponential - 20 collocation points.

A possible extension is to choose other basis functions from the proposed ones, with the condition that their transform must be known analytically. Ideally, the choice of basis functions should be such that their transform is as form-similar as possible to the function in the Laplace domain. When inverting tensorial functions, the evolution of each component is considered individually. If polycrystals are modeled, a large amount of Laplace inversions has to be carried out due to numerous individual crystals. In this case, Brenner *et al.* [15] proposed a simplified direct inversion which can reduce considerably the required CPU time. However, this technique is not used in this work since it reduces also the precision of the inversion and the CPU time is not a critical issue for two-phase materials.

Examples of numerical inversions As validation of the collocation method, several inversions of Laplace functions are made for which the transform is known a priori.

- $f(t) = e^{-t/2}, \qquad f^*(s) = \frac{s}{s+\frac{1}{2}}$

  This function is quite regular and results of the inversion are reported on figure B.1. For this first test, 20 collocation points are considered (noted with the sign $'+'$ on the figure B.1a). Continuous line is always the plot of the analytical functions (known in the Laplace domain, unknown and solution of this problem in the time domain). Crosses on figure B.1b are obtained from the development in series evaluated at several times. For such regular function, an excellent accuracy of this inversion is observed.

- $f(t) = H(t-2), \qquad f^*(s) = e^{-2s}$

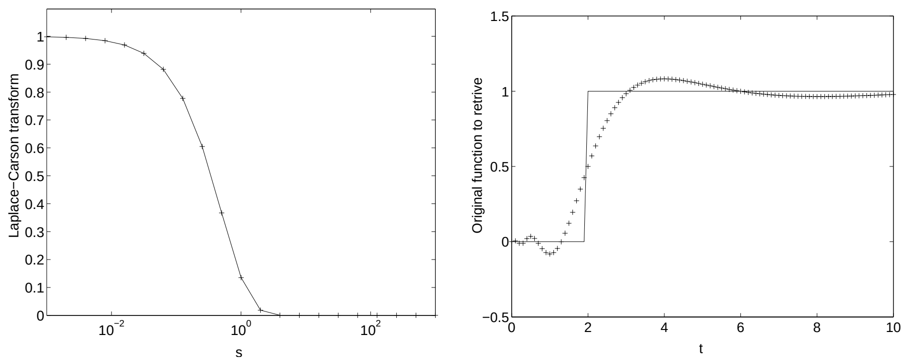

(a) Laplace domain. (b) Time domain.

Figure B.2: Numerical inversion of the transform of the step function - 20 collocation points.

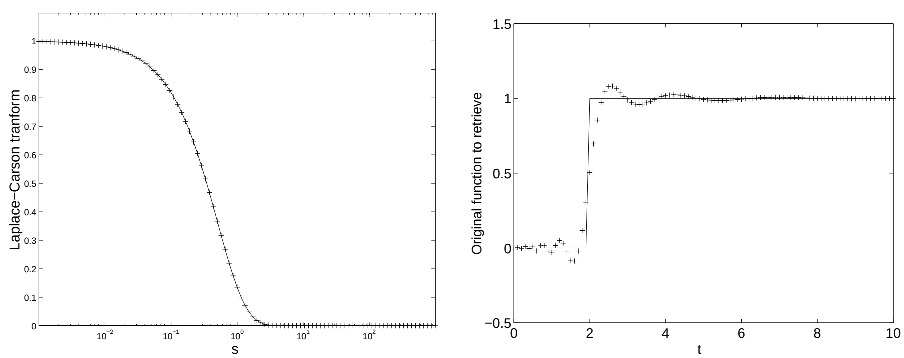

(a) Laplace domain. (b) Time domain.

Figure B.3: Numerical inversion of the transform of the step function - 100 collocation points.

A step function is now considered. At first, 20 collocation points are used for the inversion. Figure B.2b shows that the capture of the step isn't that good. When using 100 collocation points (figure B.3b) instead of 20, much better results are obtained. However, even if it might be tempting to consider as many collocation points as possible, several problems arise in this case. First one is that when rising the number of points, this increases the size of the linear system. Since solving a system of size n has a cost of n^3 operations, the complexity is growing up quickly. Another one is that increasing the size of the system leads to a singular matrix.

- $f(t) = \cos(t), \qquad f^*(s) = \frac{s^2}{s^2+1}$

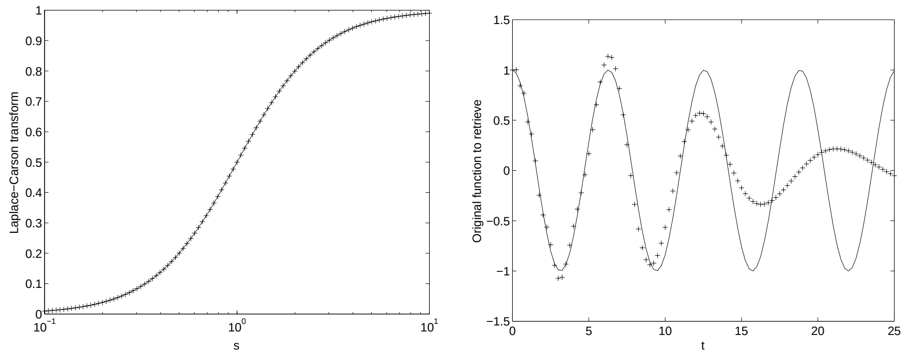

(a) Laplace domain.

(b) Time domain.

Figure B.4: Numerical inversion of the transform cosine function - 100 collocation points.

This last test considers the periodic cosine function. Figure B.4b shows that 2 complete periods are correctly captured. However, it is impossible to retrieve all the periods because basis functions considered in this case are decreasing exponentials so that the cosine function is reconstructed from balanced exponentials ! A much better choice would be to select other basis functions.

Appendix C

Incremental evaluation of a convolution product

Consider a time-dependent fourth order tensor $\boldsymbol{F}(t)$ obtained after a numerical inversion of its Laplace-Carson transform so that it is written under the form (B.2). This tensor is convoluted with a second-order tensor written in rate form $\dot{\boldsymbol{\varepsilon}}$. Such operation occurs in the computation of the macroscopic response at various times of a linear viscoelastic composite and in the localization problem of a heterogeneous elasto-viscoplastic material. Main goal of this section is to compute the convolution product at a limited memory cost. For this, consider a time interval $[t_n, t_{n+1}]$. The convolution product is already computed up to t_n and the strain history is known up to the end of the current time step ($t_{n+1} = t_n + \Delta t$). Taking into account all this information, the development hereafter enables to perform the computation of the convolution product at the end of the time step.

$$\begin{aligned}
[\boldsymbol{F} \otimes \dot{\boldsymbol{\varepsilon}}]_{(t_{n+1})} &= \int_0^{t_{n+1}} \boldsymbol{F}(t_{n+1} - u) : \dot{\boldsymbol{\varepsilon}}(u) du \\
&= \boldsymbol{A} : \int_0^{t_{n+1}} \dot{\boldsymbol{\varepsilon}}(u) du + \boldsymbol{B} : \int_0^{t_{n+1}} (t_{n+1} - u) : \dot{\boldsymbol{\varepsilon}}(u) du \\
&\quad + \int_0^{t_{n+1}} \sum_{k=1}^{M} \boldsymbol{b}_k (1 - e^{-(t_{n+1}-u)s_k}) : \dot{\boldsymbol{\varepsilon}}(u) du
\end{aligned}$$

$$
\begin{aligned}
[\boldsymbol{F} \otimes \dot{\bar{\varepsilon}}]_{(t_{n+1})} &= \left(\boldsymbol{A} + t_{n+1}\boldsymbol{B} + \sum_{k=1}^{M} \boldsymbol{b}_k\right) : (\bar{\varepsilon}(t_{n+1}) - \bar{\varepsilon}(0)) \\
& -\boldsymbol{B} : \int_0^{t_{n+1}} u\dot{\bar{\varepsilon}}(u)du \\
& -\sum_{k=1}^{M} \boldsymbol{b}_k : \int_0^{t_{n+1}} e^{-(t_{n+1}-u)s_k}\dot{\bar{\varepsilon}}(u)du,
\end{aligned} \tag{C.1}
$$

where $s_k = \frac{1}{\theta_k}$. But:

$$
\begin{aligned}
\int_0^{t_{n+1}} u\dot{\bar{\varepsilon}}(u)du &= [u\bar{\varepsilon}(u)]_0^{t_{n+1}} - \int_0^{t_{n+1}} 1\bar{\varepsilon}(u)du \\
&= t_{n+1}\bar{\varepsilon}(t_{n+1}) - \int_0^{t_{n+1}} \bar{\varepsilon}(u)du \\
&= t_{n+1}\bar{\varepsilon}(t_{n+1}) - \int_0^{t_n} \bar{\varepsilon}(u)du \\
& \quad -\frac{\Delta t}{2}(\bar{\varepsilon}(t_n) + \bar{\varepsilon}(t_{n+1})),
\end{aligned} \tag{C.2}
$$

and:

$$
\begin{aligned}
\int_0^{t_{n+1}} e^{-(t_{n+1}-u)s_k}\dot{\bar{\varepsilon}}(u)du &= \left[e^{-(t_{n+1}-u)s_k}\bar{\varepsilon}(u)\right]_0^{t_{n+1}} \\
& \quad -s_k \int_0^{t_{n+1}} e^{-(t_{n+1}-u)s_k}\bar{\varepsilon}(u)du \\
&= \bar{\varepsilon}(t_{n+1}) - e^{-t_{n+1}s_k}\bar{\varepsilon}(0) \\
& \quad -s_k \int_0^{t_{n+1}} e^{-(t_{n+1}-u)s_k}\bar{\varepsilon}(u)du.
\end{aligned} \tag{C.3}
$$

Rearranging these terms gives:

$$
\begin{aligned}
[\boldsymbol{F} \otimes \dot{\bar{\varepsilon}}]_{(t_{n+1})} &= \boldsymbol{A} : \bar{\varepsilon}(t_{n+1}) + \frac{\Delta t}{2}\boldsymbol{B} : (\bar{\varepsilon}(t_n) + \bar{\varepsilon}(t_{n+1})) \qquad \text{(C.4)} \\
& +\boldsymbol{B} : \int_0^{t_n} \bar{\varepsilon}(u)du \\
& +\sum_{k=1}^{M} s_k\boldsymbol{b}_k : \int_0^{t_{n+1}} e^{-(t_{n+1}-u)s_k}\bar{\varepsilon}(u)du \\
& -\left[\boldsymbol{A} + t_{n+1}\boldsymbol{B} + \sum_{k=1}^{M} \boldsymbol{b}_k - \sum_{k=1}^{M} \boldsymbol{b}_k e^{-t_{n+1}s_k}\right] : \bar{\varepsilon}(0).
\end{aligned}
$$

Evolving parameters from one time-step to another one are: $\boldsymbol{A}, \boldsymbol{B}, \boldsymbol{b}_k, t_{n+1}$. A last term still must be evaluated:

$$\begin{aligned}
\int_0^{t_{n+1}} e^{-(t_{n+1}-u)s_k} \bar{\varepsilon}(u) du &= \int_0^{t_n} \underbrace{e^{-(t_{n+1}-u)s_k} \bar{\varepsilon}(u)}_{e^{-(t_n+\Delta t-u)s_k} \bar{\varepsilon}(u)} du \\
&+ \int_{t_n}^{t_{n+1}} e^{-(t_{n+1}-u)s_k} \bar{\varepsilon}(u) du \\
&= e^{-\Delta t s_k} \int_0^{t_n} e^{-(t_n-u)s_k} \bar{\varepsilon}(u) du \\
&+ \int_{t_n}^{t_{n+1}} e^{-(t_{n+1}-u)s_k} \bar{\varepsilon}(u) du. \qquad \text{(C.5)}
\end{aligned}$$

In this case, using again a trapezoidal integration rule is quite bad for large values of s_k. This is due to the linear approximation of the integral containing the sharp exponential. This problem can be tackled if $\dot{\bar{\varepsilon}}(u)$ is considered as constant on each time-step. On the considered time interval, this gives:

$$\bar{\varepsilon}(u) = \bar{\varepsilon}(t_n) + (u - t_n)\dot{\bar{\varepsilon}}. \qquad \text{(C.6)}$$

Second integral in (C.5) can be rewritten as:

$$\begin{aligned}
& \int_{t_n}^{t_{n+1}} e^{-(t_{n+1}-u)s_k} \bar{\varepsilon}(u) du \\
= & \int_{t_n}^{t_{n+1}} e^{-(t_{n+1}-u)s_k} (\bar{\varepsilon}(t_n) + (u-t_n)\dot{\bar{\varepsilon}}) du \\
= & (\bar{\varepsilon}(t_n) - t_n\dot{\bar{\varepsilon}}) e^{-t_{n+1}s_k} \int_{t_n}^{t_{n+1}} e^{us_k} du + \dot{\bar{\varepsilon}} e^{-t_{n+1}s_k} \int_{t_n}^{t_{n+1}} u e^{us_k} du \\
= & (\bar{\varepsilon}(t_n) - t_n\dot{\bar{\varepsilon}}) \frac{e^{-t_{n+1}s_k}}{s_k} (e^{t_{n+1}s_k} - e^{t_n s_k}) + \dot{\bar{\varepsilon}} e^{-t_{n+1}s_k} \left[\frac{e^{us_k}}{s_k} (u - \frac{1}{s_k}) \right]_{t_n}^{t_{n+1}} \\
= & (\bar{\varepsilon}(t_n) - t_n\dot{\bar{\varepsilon}}) \frac{1 - e^{(t_n - t_{n+1})s_k}}{s_k} \\
& + \underbrace{\dot{\bar{\varepsilon}} e^{-t_{n+1}s_k} \left(\frac{e^{t_{n+1}s_k}}{s_k} (t_{n+1} - \frac{1}{s_k}) - \frac{e^{t_n s_k}}{s_k} (t_n - \frac{1}{s_k}) \right)}_{\dot{\bar{\varepsilon}} \left(\frac{1}{s_k} (t_{n+1} - \frac{1}{s_k}) - \frac{e^{(t_n - t_{n+1})s_k}}{s_k} (t_n - \frac{1}{s_k}) \right)} \\
= & \frac{1}{s_k} \left[\bar{\varepsilon}(t_n)(1 - e^{-\Delta t s_k}) + \dot{\bar{\varepsilon}} (\Delta t + \frac{e^{-\Delta t s_k} - 1}{s_k}) \right] \\
= & \frac{1}{s_k} \left[\bar{\varepsilon}(t_{n+1}) - \bar{\varepsilon}(t_n) e^{-\Delta t s_k} + (\bar{\varepsilon}(t_{n+1}) - \bar{\varepsilon}(t_n)) \frac{e^{-\Delta t s_k} - 1}{s_k \Delta t} \right]. \qquad \text{(C.7)}
\end{aligned}$$

Appendix D

Computation details of the affine formulation

D.1 Solution of the internal variables' constitutive equation

The linearized equation of internal variables is given by (6.11):

$$\dot{p}(t) = \dot{p}(t_n) + \boldsymbol{l}(\tau) : [\boldsymbol{\sigma}(t) - \boldsymbol{\sigma}(t_n)] + q(\tau)[p(t) - p(t_n)]. \tag{D.1}$$

Let's prove that the following expression is a solution of (D.1):

$$\begin{aligned} p(t) - p(t_n) &= \hat{p}(\tau, t) + \int_0^t e^{(t-u)q(\tau)} \boldsymbol{l}(\tau) : \boldsymbol{\sigma}(u) du, && \text{(D.2)} \\ \hat{p}(\tau, t) &= q^{-1}(\tau)[e^{(t-t_n)q(\tau)} - 1][\dot{p}(t_n) - \boldsymbol{l}(\tau) : \boldsymbol{\sigma}(t_n)] \\ &\quad - \int_0^{t_n} e^{(t-u)q(\tau)} \boldsymbol{l}(\tau) : \boldsymbol{\sigma}(u) du. && \text{(D.3)} \end{aligned}$$

Let's first recall the theorem which allows to switch the derivative and the integral of a function:

$$\frac{\partial}{\partial t} \int_{a(t)}^{b(t)} f(t,x) dx = \int_{a(t)}^{b(t)} \frac{\partial}{\partial t} f(t,x) dx + f(t, b(t)) \frac{d}{dt} b(t) - f(t, a(t)) \frac{d}{dt} a(t). \tag{D.4}$$

With the help of (D.4), the derivative of (D.2) is given by:

$$\begin{aligned} \dot{p}(t) &= [e^{(t-t_n)q(\tau)}][\dot{p}(t_n) - \boldsymbol{l}(\tau) : \boldsymbol{\sigma}(t_n)] + q(\tau) \int_{t_n}^t e^{(t-u)q(\tau)} \boldsymbol{l}(\tau) : \boldsymbol{\sigma}(u) du \\ &\quad + \boldsymbol{l}(\tau) : \boldsymbol{\sigma}(t). && \text{(D.5)} \end{aligned}$$

Expression of the proposed solution (D.2) can be rearranged to get an expression of the integral in function of p:

$$\begin{aligned}&\int_{t_n}^{t} e^{(t-u)q(\tau)}\boldsymbol{l}(\tau):\boldsymbol{\sigma}(u)du \\ =\ & p(t)-p(t_n)-q^{-1}(\tau)[e^{(t-t_n)q(\tau)}-1][\dot{p}(t_n)-\boldsymbol{l}(\tau):\boldsymbol{\sigma}(t_n)]. \quad \text{(D.6)}\end{aligned}$$

Inserting this result in (D.5) gives:

$$\begin{aligned}\dot{p}(t) \ =\ & [e^{(t-t_n)q(\tau)}][\dot{p}(t_n)-\boldsymbol{l}(\tau):\boldsymbol{\sigma}(t_n)]+q(\tau)(p(t)-p(t_n)) \\ & -[e^{(t-t_n)q(\tau)}-1][\dot{p}(t_n)-\boldsymbol{l}(\tau):\boldsymbol{\sigma}(t_n)]+\boldsymbol{l}(\tau):\boldsymbol{\sigma}(t). \quad \text{(D.7)}\end{aligned}$$

Rearranging the terms gives:

$$\dot{p}(t)=\boldsymbol{l}(\tau):\boldsymbol{\sigma}(t)+\dot{p}(t_n)-\boldsymbol{l}(\tau):\boldsymbol{\sigma}(t_n)+q(\tau)(p(t)-p(t_n)). \quad \text{(D.8)}$$

This result is the same as the differential equation (D.1), the proposed solution is thus acceptable. Continuity conditions are also respected:

$$\begin{aligned}\dot{p}(t=t_n) &= \dot{p}(t_n), \\ p(t=t_n) &= p(t_n). \quad \text{(D.9)}\end{aligned}$$

D.2 Linear viscoelastic expressions

The solution in $\hat{p}(\tau,t)$ of the integral equation (6.15) is inserted in equation (6.10) and gives the initial expression reported hereafter. Main goal is to rewrite such complex expression under one similar to a linear thermo-viscoelastic constitutive law by introducing the Stieljes-type convolution product. The final result is given below, a proof of the equivalence between the initial and final result is given afterwards.

Initial expression:

$$\begin{aligned}\forall t\geq t_n:\dot{\boldsymbol{\varepsilon}}^{(1)}(t) &= \boldsymbol{S}:\dot{\boldsymbol{\sigma}}(t)+\boldsymbol{m}(\tau):\boldsymbol{\sigma}(t) \\ &\quad +\boldsymbol{n}(\tau)\int_0^t e^{(t-u)q(\tau)}\boldsymbol{l}(\tau):\boldsymbol{\sigma}(u)du+\dot{\boldsymbol{\varepsilon}}^{0(1)}(\tau,t), \\ \dot{\boldsymbol{\varepsilon}}^{0(1)}(\tau,t) &= \dot{\boldsymbol{\varepsilon}}^{in}(t_n)-\boldsymbol{m}(\tau):\boldsymbol{\sigma}(t_n)+\hat{p}(\tau,t)\boldsymbol{n}(\tau). \quad \text{(D.10)}\end{aligned}$$

Final expression:

$$\dot{\boldsymbol{\varepsilon}}^{(2)}(t)=[\boldsymbol{S}_\tau\odot\dot{\boldsymbol{\sigma}}]_{(\tau,t)}+\dot{\boldsymbol{\varepsilon}}^{0(2)}(\tau,t). \quad \text{(D.11)}$$

Expressions of the creep modulus $\boldsymbol{S}_\tau$ and eigenstrain rate tensor $\dot{\boldsymbol{\varepsilon}}^0$ are:

$$\begin{aligned}
\boldsymbol{S}_\tau(\tau,t) &= \boldsymbol{S}+\boldsymbol{m}(\tau)t \\
&\quad -q^{-1}(\tau):\left[t+q^{-1}(\tau)\left(1-\boldsymbol{e}^{t\ q(\tau)}\right)\right]\boldsymbol{n}(\tau)\otimes\boldsymbol{l}(\tau), && \text{(D.12)}\\
\dot{\boldsymbol{\varepsilon}}^{0(2)}(\tau,t) &= \dot{\boldsymbol{\varepsilon}}^{in}(t_n)-\boldsymbol{m}(\tau):\boldsymbol{\sigma}(t_n)+\boldsymbol{n}(\tau)\hat{p}(\tau,t) \\
&\quad +\dot{\boldsymbol{e}}(\tau,t)[1-H(t-t_n)]+\widehat{\boldsymbol{\varepsilon}}^0(\tau,t,\boldsymbol{\sigma}(0)), && \text{(D.13)}\\
\dot{\boldsymbol{e}}(\tau,t) &= \dot{\boldsymbol{\varepsilon}}^{in}(t)-\dot{\boldsymbol{\varepsilon}}^{in}(t_n)-\boldsymbol{m}(\tau):(\boldsymbol{\sigma}(t)-\boldsymbol{\sigma}(t_n)) \\
&\quad -\boldsymbol{n}(\tau)\left[\hat{p}(\tau,t)+\int_0^t \boldsymbol{e}^{(t-u)q(\tau)}\boldsymbol{l}(\tau):\boldsymbol{\sigma}(u)du\right], && \text{(D.14)}\\
\widehat{\boldsymbol{\varepsilon}}^0(\tau,t,\boldsymbol{\sigma}(0)) &= \left[\boldsymbol{m}(\tau)-\boldsymbol{n}(\tau)q^{-1}(\tau)\boldsymbol{l}(\tau)+\boldsymbol{n}(\tau)q^{-1}(\tau)e^{tq(\tau)}\boldsymbol{l}(\tau)\right]:\boldsymbol{\sigma}(0),
\end{aligned}$$

where H is the Heavyside step function. This expression is valid for any time (later or prior to the linearization time t_n). Note that if $t \leq t_n$, expression (D.11) is reduced to:

$$\dot{\boldsymbol{\varepsilon}}(t)=\underbrace{\boldsymbol{S}:\dot{\boldsymbol{\sigma}}(t)}_{\dot{\boldsymbol{\varepsilon}}^{el}(t)}+\dot{\boldsymbol{\varepsilon}}^{in}(t). \tag{D.15}$$

Equivalence of the two expressions. In the final expression $\dot{\boldsymbol{\varepsilon}}^{0(2)}$, the Stiljes-type convolution product $\odot$ is defined as:

$$\begin{aligned}
[\boldsymbol{S}_\tau\odot\dot{\boldsymbol{\sigma}}]_{(\tau,t)} &= \frac{d}{dt}\left[\int_0^t \boldsymbol{S}_\tau(\tau,t-u):\dot{\boldsymbol{\sigma}}(u)du\right]\\
&= \int_0^t \frac{d\boldsymbol{S}_\tau}{du}(\tau,u):\dot{\boldsymbol{\sigma}}(t-u)du+\boldsymbol{S}_\tau(\tau,0):\dot{\boldsymbol{\sigma}}(t), && \text{(D.16)}
\end{aligned}$$

where the theorem (D.4) has been used to invert the derivative and the integral. Compliance terms are given by:

$$\begin{aligned}
\frac{d\boldsymbol{S}_\tau}{du}(\tau,u) &= \boldsymbol{m}(\tau)-q^{-1}(\tau)[1-q^{-1}(\tau)q(\tau)e^{uq(\tau)}]\boldsymbol{n}(\tau)\otimes\boldsymbol{l}(\tau)\\
&= \boldsymbol{m}(\tau)-q^{-1}(\tau)\boldsymbol{n}(\tau)\otimes\boldsymbol{l}(\tau)\\
&\quad +q^{-1}(\tau)e^{uq(\tau)}\boldsymbol{n}(\tau)\otimes\boldsymbol{l}(\tau), && \text{(D.17)}
\end{aligned}$$

and:

$$\boldsymbol{S}_\tau(\tau,0) = \boldsymbol{S}. \tag{D.18}$$

Expression (D.17) enables to compute the integral in (D.16). Integrals of the three terms are evaluated separately:

$$\begin{aligned}\int_0^t \boldsymbol{m}(\tau):\dot{\boldsymbol{\sigma}}(t-u)du &\underset{y=t-u}{=} -\int_t^0 \boldsymbol{m}(\tau):\dot{\boldsymbol{\sigma}}(y)dy\\ &= \int_0^t \boldsymbol{m}(\tau):\dot{\boldsymbol{\sigma}}(y)dy\\ &= \boldsymbol{m}(\tau):[\boldsymbol{\sigma}(y)]_{y=0}^{y=t}\\ &= \boldsymbol{m}(\tau):(\boldsymbol{\sigma}(t)-\boldsymbol{\sigma}(0)),\end{aligned} \tag{D.19}$$

$$\int_0^t -q^{-1}(\tau)\boldsymbol{n}(\tau)\boldsymbol{l}(\tau):\dot{\boldsymbol{\sigma}}(t-u)du = q^{-1}(\tau)\boldsymbol{n}(\tau)\boldsymbol{l}(\tau):(\boldsymbol{\sigma}(0)-\boldsymbol{\sigma}(t)), \tag{D.20}$$

$$\begin{aligned}&\int_0^t q^{-1}(\tau)e^{uq(\tau)}\boldsymbol{n}(\tau)\boldsymbol{l}(\tau):\dot{\boldsymbol{\sigma}}(t-u)du\\ &\underset{\text{by parts}}{=} [-q^{-1}(\tau)e^{uq(\tau)}\boldsymbol{n}(\tau)\boldsymbol{l}(\tau):\boldsymbol{\sigma}(t-u)]_{u=0}^{u=t}\\ &\qquad -\int_0^t q^{-1}(\tau)q(\tau)e^{uq(\tau)}\boldsymbol{n}(\tau)\boldsymbol{l}(\tau):(-\boldsymbol{\sigma}(t-u))du\\ &\underset{s\equiv t-u}{=} -q^{-1}(\tau)e^{tq(\tau)}\boldsymbol{n}(\tau)\boldsymbol{l}(\tau):\boldsymbol{\sigma}(0)+q^{-1}(\tau)e^{0.q(\tau)}\boldsymbol{n}(\tau)\boldsymbol{l}(\tau):\boldsymbol{\sigma}(t)\\ &\qquad -\int_t^0 e^{(t-s)q(\tau)}\boldsymbol{n}(\tau)\boldsymbol{l}(\tau):\boldsymbol{\sigma}(s)ds.\end{aligned} \tag{D.21}$$

Inserting all these results in the final expression (D.11) gives:

$$\begin{aligned}\dot{\boldsymbol{\varepsilon}}^{(2)}(t) \quad = \quad & \boldsymbol{S}:\dot{\boldsymbol{\sigma}}(t)+\boldsymbol{m}(\tau):\boldsymbol{\sigma}(t)-q^{-1}(\tau)\boldsymbol{n}(\tau)\boldsymbol{l}(\tau):\boldsymbol{\sigma}(t)\\ &+q^{-1}(\tau)\boldsymbol{n}(\tau)\boldsymbol{l}(\tau):\boldsymbol{\sigma}(t)+\int_0^t e^{(t-u)q(\tau)}\boldsymbol{n}(\tau)\boldsymbol{l}(\tau):\boldsymbol{\sigma}(u)du\\ &+\dot{\boldsymbol{\varepsilon}}^{in}(t_n)-\boldsymbol{m}(\tau):\boldsymbol{\sigma}(t_n)+\hat{p}(\tau,t)\boldsymbol{n}(\tau)\\ &+[1-H(t-t_n)]\Big[\dot{\boldsymbol{\varepsilon}}^{in}(t)-\dot{\boldsymbol{\varepsilon}}^{in}(t_n)-\boldsymbol{m}(\tau):(\boldsymbol{\sigma}(t)-\boldsymbol{\sigma}(t_n))\\ &\quad -\left(\hat{p}(\tau,t)+\int_0^t e^{(t-u)q(\tau)}\boldsymbol{l}(\tau):\boldsymbol{\sigma}(u)du\right)\boldsymbol{n}(\tau)\Big].\end{aligned} \tag{D.22}$$

This result is equivalent to the initial expression so that expressions (D.10) and (D.11) are the same.

D.3 Linear thermo-elastic expressions

The linear viscoelastic formulation (6.17) with eigenstrain is given by:

$$\dot{\boldsymbol{\varepsilon}}(t) = [\boldsymbol{S}_\tau \odot \dot{\boldsymbol{\sigma}}]_{(\tau,t)} + \dot{\boldsymbol{\varepsilon}}^0(\tau,t). \tag{D.23}$$

Its Laplace-Carson transform is:

$$\dot{\boldsymbol{\varepsilon}}^*(s) = \underbrace{\boldsymbol{S}^*_\tau(\tau,s)}_{\text{Term I}} : \dot{\boldsymbol{\sigma}}^*(s) + \underbrace{\dot{\boldsymbol{\varepsilon}}^{0*}(\tau,s)}_{\text{Term II}}. \tag{D.24}$$

This expression is similar to the constitutive law of a linear thermo-elastic material. Terms I and II still must be evaluated.

Term I Expression $\boldsymbol{S}_\tau(\tau,t)$ is given in equation (D.12). Its Laplace-Carson transform is:

$$\begin{aligned}
\boldsymbol{S}^*_\tau(\tau,s) &= \boldsymbol{S} + \frac{\boldsymbol{m}(\tau)}{s} - \frac{q^{-1}(\tau)\boldsymbol{n}(\tau)\otimes\boldsymbol{l}(\tau)}{s} \\
&\quad -q^{-1}(\tau)q^{-1}(\tau)\boldsymbol{n}(\tau)\otimes\boldsymbol{l}(\tau) + \frac{sq^{-1}(\tau)q^{-1}(\tau)\boldsymbol{n}(\tau)\otimes\boldsymbol{l}(\tau)}{s-q(\tau)} \\
&= \boldsymbol{S} + \frac{\boldsymbol{m}(\tau)}{s} + \frac{\boldsymbol{n}(\tau)\otimes\boldsymbol{l}(\tau)}{s(s-q(\tau))}.
\end{aligned} \tag{D.25}$$

This is valid only if $s > max(0, q(\tau)) = 0$.

Term II Expression of $\dot{\boldsymbol{\varepsilon}}^0(\tau,t)$ is given in equation (D.13). It is separated in four terms as follow:

$$\begin{aligned}
\dot{\boldsymbol{\varepsilon}}^0(\tau,t) = &\underbrace{\dot{\boldsymbol{\varepsilon}}^{in}(t_n) - \boldsymbol{m}(\tau):\boldsymbol{\sigma}(t_n)}_{\text{Term A}} + \underbrace{\hat{p}(\tau,t)\boldsymbol{n}(\tau)}_{\text{Term B}} + \underbrace{\dot{e}(\tau,t)[1-H(1-t_n)]}_{\text{Term C}} \\
&+ \underbrace{\left[\boldsymbol{m}(\tau) - \boldsymbol{n}(\tau)q^{-1}(\tau)\boldsymbol{l}(\tau) + \boldsymbol{n}(\tau)q^{-1}(\tau)e^{tq(\tau)}\boldsymbol{l}(\tau)\right]:\boldsymbol{\sigma}(0)}_{\text{Term D}}.
\end{aligned} \tag{D.26}$$

Due to the linearity of the Laplace-Carson transform, transforms of terms A, B, C and D are evaluated separately.

Term A

$$\left[\mathcal{L}(\dot{\boldsymbol{\varepsilon}}^{in}(t_n) - \boldsymbol{m}(\tau):\boldsymbol{\sigma}(t_n))\right]_{(s)} = \dot{\boldsymbol{\varepsilon}}^{in}(t_n) - \boldsymbol{m}(\tau):\boldsymbol{\sigma}(t_n). \tag{D.27}$$

Term B

$$\left[\mathcal{L}(\hat{p}(\tau,t)\boldsymbol{n}(\tau))\right]_{(s)} = p^*(\tau,s)\boldsymbol{n}(\tau). \tag{D.28}$$

Expression of $\hat{p}(\tau,t)$ is given by equation (6.16). Transform of the last term of $\hat{p}(\tau,t)$ is given by:

$$\begin{aligned} s & \int_0^\infty \int_0^{t_n} e^{(t-u)q(\tau)} \boldsymbol{l}(\tau) : \boldsymbol{\sigma}(u) du e^{-st} dt \\ = & \int_0^{t_n} s \int_0^\infty e^{t(q(\tau)-s)-uq(\tau)} dt \boldsymbol{l}(\tau) : \boldsymbol{\sigma}(u) du \\ = & -\frac{s}{q(\tau)-s} \boldsymbol{l}(\tau) : \int_0^{t_n} e^{-uq(\tau)} \boldsymbol{\sigma}(u) du. \end{aligned} \tag{D.29}$$

This is valid if $s > q(\tau)$. The transform of $\hat{p}(\tau,t)$ is given by:

$$\begin{aligned} \hat{p}^*(\tau,s)\boldsymbol{n}(\tau) = & \; q^{-1}(\tau)\frac{s}{s-q(\tau)} e^{-t_n q(\tau)} \dot{p}(t_n)\boldsymbol{n}(\tau) \\ & -q^{-1}(\tau)\frac{s}{s-q(\tau)} e^{-t_n q(\tau)} \boldsymbol{l}(\tau) : \boldsymbol{\sigma}(t_n)\, \boldsymbol{n}(\tau) \\ & -q^{-1}(\tau)\dot{p}(t_n)\boldsymbol{n}(\tau) + q^{-1}(\tau)\boldsymbol{l}(\tau) : \boldsymbol{\sigma}(t_n)\, \boldsymbol{n}(\tau) \\ & +\frac{s}{q(t_n)-s}\boldsymbol{l}(\tau) : \int_0^{t_n} e^{-uq(\tau)} \boldsymbol{\sigma}(u) du \boldsymbol{n}(\tau). \end{aligned} \tag{D.30}$$

Term C Laplace-Carson transform of term C is now examined. Expression of $\dot{e}(\tau,t)$ is given by equation (D.14). Due to the Heavyside function, integral of the Laplace-Carson transform is limited up to $t = t_n$ instead of $t = \infty$ and will be denoted:

$$\left[\mathcal{L}^{0\to t_n}(\dot{\boldsymbol{\varepsilon}}^{in}(t))\right]_{(s)} = s\int_0^{t_n} \dot{\boldsymbol{\varepsilon}}^{in}(t) e^{-st} dt. \tag{D.31}$$

Transform of several terms of $\dot{e}(\tau,t)$ can be easily evaluated:

$$\begin{aligned} \left[\mathcal{L}^{0\to t_n}(\dot{\boldsymbol{\varepsilon}}(t_n))\right]_{(s)} &= s\int_0^{t_n} \dot{\boldsymbol{\varepsilon}}^{in}(t_n) e^{-st} dt \\ &= s\dot{\boldsymbol{\varepsilon}}^{in}(t_n)\left[\frac{-e^{-st}}{s}\right]_0^{t_n} \\ &= \dot{\boldsymbol{\varepsilon}}^{in}(t_n)(1-e^{-st_n}), \\ \left[\mathcal{L}^{0\to t_n}(\boldsymbol{m}(\tau):\boldsymbol{\sigma}(t))\right]_{(s)} &= s\boldsymbol{m}(\tau) : \int_0^{t_n} \boldsymbol{\sigma}(t) e^{-st} dt, \\ \left[\mathcal{L}^{0\to t_n}(\boldsymbol{m}(\tau):\boldsymbol{\sigma}(t_n))\right]_{(s)} &= \boldsymbol{m}(\tau) : \boldsymbol{\sigma}(t_n)(1-e^{-st_n}), \\ \left[\mathcal{L}^{0\to t_n}(\boldsymbol{n}(\tau)\hat{p}(\tau,t))\right]_{(s)} &= \boldsymbol{n}(\tau)\left[\mathcal{L}^{0\to t_n}(\hat{p}(\tau,t))\right]_{(s)}. \end{aligned} \tag{D.32}$$

In this last equation, things are becoming a little bit more complex since $\hat{p}(\tau,t)$ is given by equation (6.16):

$$\begin{aligned}\hat{p}(\tau,t) &= q^{-1}(\tau)\left[e^{(t-t_n)q(\tau)}-1\right][\dot{p}(t_n)-\boldsymbol{l}(\tau):\boldsymbol{\sigma}(t_n)] \\ &\quad -\int_0^{t_n} e^{(t-u)q(\tau)}\boldsymbol{l}(\tau):\boldsymbol{\sigma}(u)du. \qquad \text{(D.33)}\end{aligned}$$

Firstly, let's evaluate a preliminary integral:

$$\begin{aligned}\left[\mathcal{L}^{0\to t_n}(e^{(t-t_n)q(\tau)})\right]_{(s)} &= s\int_0^{t_n} e^{(t-t_n)q(\tau)}e^{-st}dt \\ &= s\int_0^{t_n} e^{(q(\tau)-s)t}e^{-t_nq(\tau)}dt \\ &= s\left[\frac{e^{(q(\tau)-s)t}e^{-t_nq(\tau)}}{q(\tau)-s}\right]_0^{t_n} \\ &= s\frac{e^{-st_n}-e^{-q(\tau)t_n}}{q(\tau)-s}. \qquad \text{(D.34)}\end{aligned}$$

This gives the transform of the last term of $\hat{p}(\tau,t)$:

$$\begin{aligned}& s \int_0^{t_n}\int_0^{t_n} e^{(t-u)q(\tau)}\boldsymbol{l}(\tau):\boldsymbol{\sigma}(u)due^{-st}dt \\ =& \int_0^{t_n} s\int_0^{t_n} e^{(t-u)q(\tau)}e^{-st}dt\boldsymbol{l}(\tau):\boldsymbol{\sigma}(u)du \\ =& \int_0^{t_n} s\left[\frac{e^{t(q(\tau)-s)-uq(\tau)}}{q(\tau)-s}\right]_0^{t_n}\boldsymbol{l}(\tau):\boldsymbol{\sigma}(u)du \\ =& \int_0^{t_n}\frac{s}{q(\tau)-s}(e^{t_n(q(\tau)-s)-uq(\tau)}-e^{-uq(\tau)})\boldsymbol{l}(\tau):\boldsymbol{\sigma}(u)du \\ =& \frac{s}{q(\tau)-s}\boldsymbol{l}(\tau):\int_0^{t_n} e^{-uq(\tau)}\boldsymbol{\sigma}(u)du\,(e^{t_n(q(\tau)-s)}-1). \qquad \text{(D.35)}\end{aligned}$$

Finally, the modified Laplace-Carson transform of (D.32) is given by:

$$\begin{aligned}&\left[\mathcal{L}^{0\to t_n}(\hat{p}(\tau,t)\boldsymbol{n}(\tau))\right]_{(s)} = q^{-1}(\tau)s\frac{e^{-st_n}-e^{-q(\tau)t_n}}{q(\tau)-s}\dot{p}(t_n)\boldsymbol{n}(\tau) \\ &-q^{-1}(\tau)s\frac{e^{-st_n}-e^{-q(\tau)t_n}}{q(\tau)-s}\boldsymbol{l}(\tau):\boldsymbol{\sigma}(t_n)\boldsymbol{n}(\tau) \\ &+\frac{s}{q(\tau)-s}\boldsymbol{l}(\tau):\int_0^{t_n} e^{-uq(\tau)}\boldsymbol{\sigma}(u)du\,(e^{t_n(q(\tau)-s)}-1)\boldsymbol{n}(\tau).\end{aligned}$$

Last term of (D.14) can be transformed as:

$$\begin{aligned} & \left[\mathcal{L}^{0\to t_n}\boldsymbol{l}(\tau):\int_0^t e^{(t-u)q(\tau)}\boldsymbol{\sigma}(u)du\boldsymbol{n}(\tau)\right]_{(s)} \\ = \quad & s\int_0^{t_n}\boldsymbol{l}(\tau):\int_0^t e^{(t-u)q(\tau)}\boldsymbol{\sigma}(u)du\,e^{-st}dt\boldsymbol{n}(\tau). \end{aligned} \tag{D.36}$$

Regrouping all the partial transform, one get the one of $\dot{e}(\tau,t)$:

$$\begin{aligned} & [\mathcal{L}(\dot{e}(\tau,t)[1-H(t-t_n)])]_{(s)} \\ = \quad & s\int_0^{t_n}\dot{\boldsymbol{\varepsilon}}^{in}(t)e^{-st}dt-\dot{\boldsymbol{\varepsilon}}^{in}(t_n)(1-e^{-st_n})-s\boldsymbol{m}(\tau):\int_0^{t_n}\boldsymbol{\sigma}(t)e^{-st}dt \\ & +\boldsymbol{m}(\tau):\boldsymbol{\sigma}(t_n)(1-e^{-st_n}) \\ & -q^{-1}(\tau)s\frac{e^{-st_n}-e^{-q(\tau)t_n}}{q(\tau)-s}\dot{p}(t_n)\boldsymbol{n}(\tau) \\ & +q^{-1}(\tau)\boldsymbol{l}(\tau):\boldsymbol{\sigma}(t_n)s\frac{e^{-st_n}-e^{-q(\tau)t_n}}{q(\tau)-s}\boldsymbol{n}(\tau) \\ & +q^{-1}(\tau)\left[\dot{p}(t_n)-\boldsymbol{l}(\tau):\boldsymbol{\sigma}(t_n)\right]\boldsymbol{n}(\tau)(1-e^{-st_n}) \\ & +\frac{s}{q(\tau)-s}\boldsymbol{l}(\tau):\int_0^{t_n}e^{-uq(\tau)}\boldsymbol{\sigma}(u)du\,(e^{t_n(q(\tau)-s)}-1)\boldsymbol{n}(\tau) \qquad \text{(D.37)} \\ & -s\boldsymbol{n}(\tau):\boldsymbol{l}(\tau)\int_0^{t_n}\int_0^t e^{(t-u)q(\tau)}\boldsymbol{\sigma}(u)du\,e^{-st}dt. \qquad \text{(D.38)} \end{aligned}$$

Last term (D.37) can be rewritten as:

$$\begin{aligned} & \boldsymbol{n}(\tau):\boldsymbol{l}(\tau)\int_0^{t_n}\int_0^t e^{(t-u)q(\tau)}\boldsymbol{\sigma}(u)\,du\,e^{-st}\,dt \qquad \text{(D.39)} \\ = \quad & \frac{s\boldsymbol{n}(\tau):\boldsymbol{l}(\tau)}{q(\tau)-s}\left[e^{t_n(q(\tau)-s)}\int_0^{t_n}\boldsymbol{\sigma}(u)e^{-uq(\tau)}\,du-\int_0^{t_n}\boldsymbol{\sigma}(u)e^{-su}\,du\right]. \end{aligned}$$

This enable to further simplify the sum of (D.37) and (D.38).

Term D Term D can be viewed as a function of $\boldsymbol{\sigma}(0)$. Its Laplace-Carson transform is given by:

$$\begin{aligned} \hat{\boldsymbol{\varepsilon}}^{0*}(\tau,s,\boldsymbol{\sigma}(0)) \quad = \quad & \boldsymbol{m}(\tau):\boldsymbol{\sigma}(0)-\boldsymbol{n}(\tau)q^{-1}(\tau)\boldsymbol{l}(\tau):\boldsymbol{\sigma}(0) \\ + \quad & \boldsymbol{n}(\tau)q^{-1}(\tau)\frac{s}{s-q(\tau)}\boldsymbol{l}(\tau):\boldsymbol{\sigma}(0). \end{aligned} \tag{D.40}$$

This is valid only if $s>q(\tau)$. Regrouping terms A, B, C and D enables to compute $\dot{\boldsymbol{\varepsilon}}^{0*}$. Its final expression is reported in the main text (section 6.3.1).

D.4 Limit values for the Laplace-Carson inversion

For the numerical inversion of the Laplace-Carson transform with a collocation method, two limits of the function are needed. For a function $f(t)$ (denoted $f^*(s)$ in the Laplace domain), these can be evaluated equivalently in the Laplace or time domain:

$$\begin{aligned} \lim_{s\to\infty} f^*(s) &= \lim_{t\to 0} f(t), \\ \lim_{s\to 0} s f^*(s) &= \lim_{t\to\infty} \frac{f(t)}{t}. \end{aligned} \tag{D.41}$$

In the proposed algorithm to solve the localization problem for two-phase elasto-viscoplastic plastic composite with an affine formulation, the two strain concentration tensors of linear thermo-elasticity have to be inverted: $\boldsymbol{A}^{\epsilon *}(\tau, s)$ and $\boldsymbol{a}^{\epsilon *}(\tau, s)$. Expressions for the strain concentration tensors used in this section correspond to the Mori-Tanaka homogenization scheme (section 4.2.3) but limit values for other mean-field models can be obtained in a similar way. If the final macroscopic response is computed via the macroscopic relation of linear viscoelasticity (equation (6.24)), macroscopic stiffness and eigenstrain must also be inverted. Limit values of these expressions are given in Pierard [77].

D.4.1 The different functions

In the following, the subscript r refers to the matrix ($r = 0$) or the inclusions ($r = 1$).

General case $\boldsymbol{C}_0^*(\tau, s) \neq \boldsymbol{C}_1^*(\tau, s)$

$$\begin{aligned} \boldsymbol{S}_r^*(\tau, s) &= \boldsymbol{S}_r + \frac{\boldsymbol{m}_r(\tau)}{s} + \frac{\boldsymbol{n}_r(\tau) \otimes \boldsymbol{l}_r(\tau)}{s(s - q_r(\tau))}, \\ \boldsymbol{C}_r^*(\tau, s) &= \boldsymbol{S}_r^{*\,-1}(\tau, s), \\ \mathcal{E}^*(\tau, s) &: \text{Eshelby's tensor remains finite for any } \nu \neq 0, \\ \boldsymbol{B}^{\epsilon *}(\tau, s) &= \left[\boldsymbol{I} + \mathcal{E}^*(\tau, s) : \left((\boldsymbol{C}_0^*(\tau, s))^{-1} : \boldsymbol{C}_1^*(\tau, s) - \boldsymbol{I}\right)\right]^{-1}, \\ \boldsymbol{A}^{\epsilon *}(\tau, s) &= \boldsymbol{B}^{\epsilon *}(\tau, s) : \left[(1 - v_1)\boldsymbol{I} + v_1 \boldsymbol{B}^{\epsilon *}(\tau, s)\right]^{-1}, \\ \boldsymbol{\varepsilon}_r^{0*}(\tau, s) &: \text{see equation (6.21)}, \\ \boldsymbol{a}^{\epsilon *}(\tau, s) &= (\boldsymbol{A}^{\epsilon *} - \boldsymbol{I}) : (\boldsymbol{C}_1^*(\tau, s) - \boldsymbol{C}_0^*(\tau, s))^{-1} \\ &\quad : [\boldsymbol{C}_0^*(\tau, s) : \boldsymbol{\varepsilon}_0^{0*}(\tau, s) - \boldsymbol{C}_1^*(\tau, s) : \boldsymbol{\varepsilon}_1^{0*}(\tau, s)]. \end{aligned} \tag{D.42}$$

Particular case Some of these expressions become invalid and have to be reformulated if $\boldsymbol{C}_1^*(\tau,s)=\boldsymbol{C}_0^*(\tau,s)$

$$\begin{aligned}
&\boldsymbol{S}_r^*(\tau,s),\boldsymbol{C}_0^*(\tau,s) \text{ and } \mathcal{E}(\tau,s) \text{ remain valid and unchanged,}\\
&\boldsymbol{B}^{\epsilon*}(\tau,s)=\boldsymbol{I},\\
&\boldsymbol{A}^{\epsilon*}(\tau,s)=\boldsymbol{I},\\
&\boldsymbol{\varepsilon}^{0*}(\tau,s) \text{ remains valid and unchanged,}\\
&\boldsymbol{a}^{\epsilon*}(\tau,s) \text{ becomes invalid.}
\end{aligned} \tag{D.43}$$

In the last expression, when the inclusion's parameters tend to the ones of the matrix, first term of $\boldsymbol{a}^{\epsilon*}(\tau,s)$ tends to $\boldsymbol{I}$, second one to $\boldsymbol{0}$ and the contraction of the third and fourth ones tends to $\boldsymbol{\varepsilon}_1^{0*}(\tau,s)-\boldsymbol{\varepsilon}_0^{0*}(\tau,s)$. Thus, if $\boldsymbol{C}_0^*(\tau,s)=\boldsymbol{C}_1^*(\tau,s)$, $\boldsymbol{a}^{\epsilon*}(\tau,s)=\boldsymbol{0}$.

D.4.2 Limit values for $s\to\infty$

General case $\lim_{s\to\infty}\boldsymbol{C}_0^*(\tau,s)\neq\lim_{s\to\infty}\boldsymbol{C}_1^*(\tau,s)$

$$\begin{aligned}
\lim_{s\to\infty}\boldsymbol{S}_r^*(\tau,s) &= \boldsymbol{S}_r,\\
\lim_{s\to\infty}\boldsymbol{C}_r^*(\tau,s) &= \boldsymbol{S}_r^{-1},\\
\lim_{s\to\infty}\mathcal{E}^*(\tau,s) &\quad \text{remains finite,}\\
\lim_{s\to\infty}\boldsymbol{B}^{\epsilon*}(\tau,s) &= \left[\boldsymbol{I}+\lim_{s\to\infty}\mathcal{E}^*:(\boldsymbol{S}_0:\boldsymbol{S}_1^{-1}-\boldsymbol{I})\right]^{-1},\\
\lim_{s\to\infty}\boldsymbol{A}^{\epsilon*}(\tau,s) &= \lim_{s\to\infty}\boldsymbol{B}^{\epsilon*}(\tau,s):(v_1\lim_{s\to\infty}\boldsymbol{B}^{\epsilon*}(\tau,s)+(1-v_1)\boldsymbol{I})^{-1},\\
\lim_{s\to\infty}\boldsymbol{\varepsilon}_r^{0*}(\tau,s) &= \boldsymbol{m}_r(\tau):\boldsymbol{\sigma}_r(0),\\
\lim_{s\to\infty}\boldsymbol{a}^{\epsilon*}(\tau,s) &= (1-v_1)\left(v_1\lim_{s\to\infty}\boldsymbol{B}^{\epsilon*}(\tau,s)+(1-v_1)\boldsymbol{I}\right)^{-1},\\
&\quad :\left(\lim_{s\to\infty}\boldsymbol{B}^{\epsilon*}(\tau,s)-\boldsymbol{I}\right):(\boldsymbol{S}_1^{-1}-\boldsymbol{S}_0^{-1})^{-1},\\
&\quad :\left(\boldsymbol{S}_0^{-1}:\boldsymbol{m}_0(\tau):\boldsymbol{\sigma}_0(0)-\boldsymbol{S}_1^{-1}:\boldsymbol{m}_1(\tau):\boldsymbol{\sigma}_1(0)\right).
\end{aligned} \tag{D.44}$$

Limits of the strain concentration tensors can be evaluated just once for all time-steps if $\boldsymbol{\sigma}_0(0)=0$ and $\boldsymbol{\sigma}_1(0)=0$. Otherwise, additional time-dependent terms must be considered.

Particular case $\lim_{s\to\infty}\boldsymbol{C}_0^*(\tau,s)=\lim_{s\to\infty}\boldsymbol{C}_1^*(\tau,s)$

$\lim_{s\to\infty} \boldsymbol{S}_r^*(\tau,s)$ and $\lim_{s\to\infty} \boldsymbol{C}_r^*(\tau,s)$ remains valid and unchanged.

$$\begin{aligned}
\lim_{s\to\infty} \mathcal{E}^*(\tau,s) & \quad \text{(remains finite)},\\
\lim_{s\to\infty} \boldsymbol{B}^{\epsilon *}(\tau,s) &= \boldsymbol{I} \text{ (simplified)},\\
\lim_{s\to\infty} \boldsymbol{A}^{\epsilon *}(\tau,s) &= \boldsymbol{I} \text{ (simplified)},\\
\lim_{s\to\infty} \boldsymbol{\varepsilon}_r^{0*}(\tau,s) &= \boldsymbol{m}_r(\tau) : \boldsymbol{\sigma}_r(0) \text{ (unchanged)},\\
\lim_{s\to\infty} \boldsymbol{a}^{\epsilon *}(\tau,s) &= \boldsymbol{0} \text{ (undetermined in the general case)}. \qquad \text{(D.45)}
\end{aligned}$$

D.4.3 Limit values for $s \to 0$

General case $\lim_{s\to 0} \boldsymbol{C}_0^*(\tau,s) \neq \lim_{s\to 0} \boldsymbol{C}_1^*(\tau,s)$

$$\begin{aligned}
\lim_{s\to 0} \boldsymbol{S}_r^*(\tau,s) &= \frac{1}{s(s-q_r(\tau))}[s(s-q_r(\tau))\boldsymbol{S}_r\\
&\qquad +(s-q_r(\tau))\boldsymbol{m}_r(\tau)+\boldsymbol{n}_r(\tau)\otimes \boldsymbol{l}_r(\tau)],\\
\lim_{s\to 0} \boldsymbol{C}_r^*(\tau,s) &= \left[\lim_{s\to 0} \boldsymbol{S}_r^*(\tau,s)\right]^{-1}\\
&= \lim_{s\to 0} -sq_r(\tau)\left[-q_r(\tau)\boldsymbol{m}_0(\tau)+\boldsymbol{n}_r(\tau)\otimes \boldsymbol{l}_r(\tau)\right]^{-1}\\
&= \boldsymbol{0},\\
\lim_{s\to 0} \mathcal{E}^*(\tau,s) & \quad \text{remains finite since } \lim_{s\to 0} \boldsymbol{C}_0^*(\tau,s)=0,
\end{aligned}$$

$$\begin{aligned}
& \lim_{s\to 0}\left[\boldsymbol{C}_0^{*\,-1}(\tau,s) : \boldsymbol{C}_1^*(\tau,s)-\boldsymbol{I}\right]\\
=\ & \lim_{s\to 0} \frac{q_1(\tau)}{q_0(\tau)}\left[s(s-q_0(\tau))\boldsymbol{S}_0+(s-q_0(\tau))\boldsymbol{m}_0(\tau)+\boldsymbol{n}_0(\tau)\otimes \boldsymbol{l}_0(\tau)\right] :\\
& \quad : \left[s(s-q_1(\tau))\boldsymbol{S}_1+(s-q_1(\tau))\boldsymbol{m}_1(\tau)+\boldsymbol{n}_1(\tau)\otimes \boldsymbol{l}_1(\tau)\right]^{-1}-\boldsymbol{I}\\
=\ & \frac{q_1(\tau)}{q_0(\tau)}\left[\boldsymbol{n}_0(\tau)\otimes \boldsymbol{l}_0(\tau)-q_0(\tau)\boldsymbol{m}_0(\tau)\right] : \left[\boldsymbol{n}_1(\tau)\otimes \boldsymbol{l}_1(\tau)-q_1(\tau)\boldsymbol{m}_1(\tau)\right]^{-1}\\
& \quad -\boldsymbol{I}. \qquad \text{(D.46)}
\end{aligned}$$

$$\begin{aligned}
\lim_{s\to 0} \boldsymbol{B}^{\epsilon *}(\tau,s) &= \underbrace{\lim_{s\to 0}\left[\boldsymbol{I}+\underbrace{\boldsymbol{S}^*(\boldsymbol{I},\boldsymbol{C}^{*\,iso}(\tau,s))}_{\text{Finite}} : \underbrace{(\boldsymbol{C}_0^{*\,-1} : \boldsymbol{C}_1^*-\boldsymbol{I})}_{\text{Finite}}\right]^{-1}}_{\text{Finite}}.\\
\lim_{s\to 0} s\boldsymbol{A}^{\epsilon *}(\tau,s) &= s\underbrace{\lim_{s\to 0} \boldsymbol{H}^{\boldsymbol{\varepsilon}\,*}(\tau,s)}_{\text{Finite}} : \underbrace{[v_0\boldsymbol{I}+v_1\underbrace{\lim_{s\to 0} \boldsymbol{H}^{\boldsymbol{\varepsilon}\,*}(\tau,s)}_{\text{Finite}}]^{-1}}_{\text{Finite}}\\
&= \boldsymbol{0}. \qquad \text{(D.47)}
\end{aligned}$$

$$
\begin{aligned}
\lim_{s\to 0}\boldsymbol{\varepsilon}_r^{0*}(\tau,s) &= \dot{\boldsymbol{\varepsilon}}_r^{in}(\tau) - q^{-1}(\tau)\dot{p}(\tau)\boldsymbol{n}(\tau) + q^{-1}(\tau)\boldsymbol{l}(\tau):\boldsymbol{\sigma}(\tau)\boldsymbol{n}(\tau) \\
&- \left(\int_0^\tau e^{(\tau-t)q(\tau)}\boldsymbol{l}(\tau):\boldsymbol{\sigma}(t)dt\right)\boldsymbol{n}(\tau) \\
&+ \boldsymbol{m}(\tau):\boldsymbol{\sigma}(0) - \boldsymbol{n}(\tau)q^{-1}(\tau)\boldsymbol{l}(\tau):\boldsymbol{\sigma}(0). \qquad \text{(D.48)}
\end{aligned}
$$

Remains finite!

$$
\begin{aligned}
&\lim_{s\to 0}\left[\boldsymbol{C}_1^*(\tau,s)-\boldsymbol{C}_0^*(\tau,s)\right]^{-1}:\left[\boldsymbol{C}_0^*(\tau,s):\boldsymbol{\varepsilon}_0^{0*}(\tau,s)-\boldsymbol{C}_1^*(\tau,s):\boldsymbol{\varepsilon}_1^{0*}(\tau,s)\right] \\
&= \lim_{s\to 0} s^{-1}[-q_1(\tau)\left(-q_1(\tau)\boldsymbol{m}_1(\tau)+\boldsymbol{n}_1(\tau)\otimes\boldsymbol{l}_1(\tau)\right)^{-1} \\
&\quad +q_0(\tau)\left(-q_0(\tau)\boldsymbol{m}_0(\tau)+\boldsymbol{n}_0(\tau)\otimes\boldsymbol{l}_0(\tau)\right)^{-1}]^{-1} \\
&: s[-q_0(\tau)\left(-q_0(\tau)\boldsymbol{m}_0(\tau)+\boldsymbol{n}_0(\tau)\otimes\boldsymbol{l}_0(\tau)\right)^{-1}:\boldsymbol{\varepsilon}_0^{0*} \\
&\quad +q_1(\tau)\left(-q_1(\tau)\boldsymbol{m}_1(\tau)+\boldsymbol{n}_1(\tau)\otimes\boldsymbol{l}_1(\tau)\right)^{-1}:\boldsymbol{\varepsilon}_1^{0*}]. \qquad \text{(D.49)}
\end{aligned}
$$

s^{-1} and s can be simplified each others and this limit is thus finite.

$$
\begin{aligned}
\lim_{s\to 0} s\boldsymbol{a}^{\epsilon*}(\tau,s) &= sv_0\underbrace{\left[v_1\lim_{s\to 0}\boldsymbol{B}^{\epsilon*}(\tau,s)+v_0\boldsymbol{I}\right]^{-1}}_{\text{Finite}}:\underbrace{\left[\lim_{s\to 0}\boldsymbol{B}^{\epsilon*}(\tau,s)-\boldsymbol{I}\right]}_{\text{Finite}} \\
&:\underbrace{\left[\boldsymbol{C}_1^*(\tau,s)-\boldsymbol{C}_0^*(\tau,s)\right]^{-1}:\left[\boldsymbol{C}_0^*(\tau,s):\boldsymbol{\varepsilon}_0^{0*}(\tau,s)-\boldsymbol{C}_1^*(\tau,s):\boldsymbol{\varepsilon}_1^{0*}(\tau,s)\right]}_{\text{Finite}} \\
&= \boldsymbol{0}. \qquad \text{(D.50)}
\end{aligned}
$$

The two required limits are thus nil for all times.

Particular case $\lim_{s\to 0}\boldsymbol{C}_0^*(\tau,s)=\lim_{s\to 0}\boldsymbol{C}_1^*(\tau,s)$.

$\lim_{s\to 0}\boldsymbol{S}_r^*(\tau,s)$, $\lim_{s\to 0}\boldsymbol{C}_r^*(\tau,s)$ and $\lim_{s\to 0}\mathcal{E}^*(\boldsymbol{I},\boldsymbol{C}^{*\,iso}(\tau,s))$ remain valid and unchanged.

$$
\begin{aligned}
\lim_{s\to 0}\boldsymbol{H}^{\boldsymbol{\varepsilon}\,*}(\tau,s) &= \boldsymbol{I}, \\
\lim_{s\to 0}s\boldsymbol{F}^*(\tau,s) &= \boldsymbol{0}\ \text{(unchanged)}, \\
\lim_{s\to 0}\boldsymbol{\varepsilon}_r^{0*}(\tau,s) &\quad\ \text{(unchanged)}, \\
\lim_{s\to 0}s\boldsymbol{a}^{\epsilon*}(\tau,s) &= \boldsymbol{0}\ \text{(unchanged)}\ . \qquad \text{(D.51)}
\end{aligned}
$$

Appendix E

Tensile tests

This appendix examines the required additional loop for tensile test. This is necessary when considering loading cases such as uniaxial tension, biaxial tension, hydrostatic pressure, creep,... Only the two first cases are examined here. The proposed algorithm is for a strain driven approach so that imposition of the required conditions on the stress tensor is not trivial a priori. For example, in the case of a tensile test, $\Delta\varepsilon_{11}$ is given over a time step (if traction is performed along direction 1) but the other components of the strain increment are unknown. This iterative procedure is required at each time step. Hereafter, $\boldsymbol{C}$ designates the tangent modulus.

E.1 Uniaxial tensile test

At the end of a time-step, the system should be form similar to:

$$\begin{pmatrix} \Delta\sigma_{11} & 0 & 0 \\ 0 & 0 & 0 \\ 0 & 0 & 0 \end{pmatrix} = \bar{\boldsymbol{C}} : \begin{pmatrix} \Delta\varepsilon_{11} & 0 & 0 \\ 0 & \Delta\varepsilon_{22} & 0 \\ 0 & 0 & \Delta\varepsilon_{33} \end{pmatrix},$$

$\Delta\sigma_{22}$ and $\Delta\sigma_{33}$ are nil only for particular values of the unknowns $\Delta\varepsilon_{22}$ and $\Delta\varepsilon_{33}$. Starting form arbitrary values for these components, an iterate Newton-Raphson scheme is used. The two functions to varnish are written as:

$$\begin{aligned} \Delta\sigma_{22} &= \bar{C}_{2211}\Delta\varepsilon_{11} + \bar{C}_{2222}\Delta\varepsilon_{22} + \bar{C}_{2233}\Delta\varepsilon_{33} = 0, \\ \Delta\sigma_{33} &= \bar{C}_{3311}\Delta\varepsilon_{11} + \bar{C}_{3322}\Delta\varepsilon_{22} + \bar{C}_{3333}\Delta\varepsilon_{33} = 0. \end{aligned} \tag{E.1}$$

The Newton-Raphson system can thus be written as:

$$\begin{bmatrix} \Delta\sigma_{22} \\ \Delta\sigma_{33} \end{bmatrix}^{it} + \begin{bmatrix} \bar{C}_{2222} & \bar{C}_{2233} \\ \bar{C}_{3322} & \bar{C}_{3333} \end{bmatrix}^{it} : \begin{bmatrix} \Delta\varepsilon_{22}^{it+1} - \Delta\varepsilon_{22}^{it} \\ \Delta\varepsilon_{33}^{it+1} - \Delta\varepsilon_{33}^{it} \end{bmatrix} = 0.$$

$\Delta\varepsilon_{33}^{it+1}$ can be isolated from the first equation:

$$\Delta\varepsilon_{33}^{it+1} = \Delta\varepsilon_{33}^{it} - \frac{1}{\bar{C}_{2233}^{it}}\Delta\sigma_{22}^{it} - \frac{1}{\bar{C}_{2233}^{it}}\bar{C}_{2222}^{it}(\Delta\varepsilon_{22}^{it+1} - \Delta\varepsilon_{22}^{it}). \tag{E.2}$$

Inserting this result into the second one gives:

$$\Delta\sigma_{33}^{it} + \bar{C}_{3322}^{it}(\Delta\varepsilon_{22}^{it+1} - \Delta\varepsilon_{22}^{it}) - C_{3333}^{it}\left(\frac{\Delta\sigma_{22}^{it}}{C_{2233}^{it}} + \frac{C_{2222}^{it}}{C_{2233}^{it}}(\Delta\varepsilon_{22}^{it+1} - \Delta\varepsilon_{22}^{it})\right) = 0,$$

which can be rewritten as:

$$(\Delta\varepsilon_{22}^{it+1} - \Delta\varepsilon_{22}^{it})\left(\bar{C}_{3322}^{it} - \frac{C_{3333}^{it}C_{2222}^{it}}{C_{2233}^{it}}\right) + \Delta\sigma_{33}^{it} - \frac{C_{3333}^{it}}{C_{2233}^{it}}\Delta\sigma_{22}^{it} = 0. \tag{E.3}$$

Final expression of the new iteration of the strain increments are given by:

$$\begin{aligned}
\Delta\varepsilon_{22}^{it+1} &= \Delta\varepsilon_{22}^{it} + \left(\bar{C}_{3322}^{it} - \frac{C_{3333}^{it}C_{2222}^{it}}{C_{2233}^{it}}\right)^{-1}\left(\frac{C_{3333}^{it}}{C_{2233}^{it}}\Delta\sigma_{22}^{it} - \Delta\sigma_{33}^{it}\right), \\
\Delta\varepsilon_{33}^{it+1} &= \Delta\varepsilon_{33}^{it} - \frac{\Delta\sigma_{22}^{it}}{\bar{C}_{2233}^{it}} - \frac{\bar{C}_{2222}^{it}}{\bar{C}_{2233}^{it}}(\Delta\varepsilon_{22}^{it+1} - \Delta\varepsilon_{22}^{it}).
\end{aligned} \tag{E.4}$$

Initialization of the strain increments can be given by:

$$\begin{aligned}
&\Delta\varepsilon_{11}^{1} \text{ given}, \\
&\Delta\varepsilon_{22}^{1} = -0.49\Delta\varepsilon_{11}^{1}, \\
&\Delta\varepsilon_{33}^{1} = -0.49\Delta\varepsilon_{11}^{1}.
\end{aligned} \tag{E.5}$$

E.2 Biaxial tensile test

At the end of a time-step, the system should be form similar to:

$$\begin{pmatrix} \Delta\sigma_{11} & 0 & 0 \\ 0 & \Delta\sigma_{22} & 0 \\ 0 & 0 & 0 \end{pmatrix} = \bar{C} : \begin{pmatrix} \Delta\varepsilon_{11} & 0 & 0 \\ 0 & \Delta\varepsilon_{22} & 0 \\ 0 & 0 & \Delta\varepsilon_{33} \end{pmatrix}.$$

Only the last component of the stress matrix is not trivially satisfied. In this case, the problem is thus reduced to find the solution of a single equation:

$$\Delta\sigma_{33} = \bar{C}_{3311} : \Delta\varepsilon_{11} + \bar{C}_{3322} : \Delta\varepsilon_{22} + \bar{C}_{3333} : \Delta\varepsilon_{33}. \tag{E.6}$$

Solving this equation with the Newton-Raphson method gives:

$$\Delta\sigma_{33}^{it} + \bar{C}_{3333} : (\Delta\varepsilon_{33}^{it+1} - \Delta\varepsilon_{33}^{it}) = 0. \tag{E.7}$$

The new iteration of the strain increment is finally given by:

$$\Delta\varepsilon_{33}^{it+1} = \Delta\varepsilon_{33}^{it} - \frac{\Delta\sigma_{33}^{it}}{\bar{C}_{3333}}. \tag{E.8}$$

Appendix F

A short introduction to Affinistan

Affinistan is the main software developed during this thesis. It enables to predict the behavior of two phase elasto-viscoplastic composites. This is done with an affine linearization of the local constitutive law and predictions are obtained with a mean-field homogenization scheme. Even if not mandatory, Affinistan comes with its graphical user interface which enables to describe easily both materials, the loading conditions and some numerical parameters. Furthermore, a basic post processor handles with plots. Possibilities offered by the software are briefly presented hereafter.

F.1 Input section

The input section is divided into four main windows (see figure F.1). First and second ones describe both phases of the material. A third one is devoted to the mean-field homogenization scheme and the loading parameters. The last section specifies some optional parameters. Furthermore, a main toolbar offers some global options.

F.1.1 Toolbar

Here is a basic description of the buttons of the main toolbar.

- New: Reinitialize all the fields as when launching the software.
- Load: Enable to load an input (.dat) file for a simulation with Affinistan.

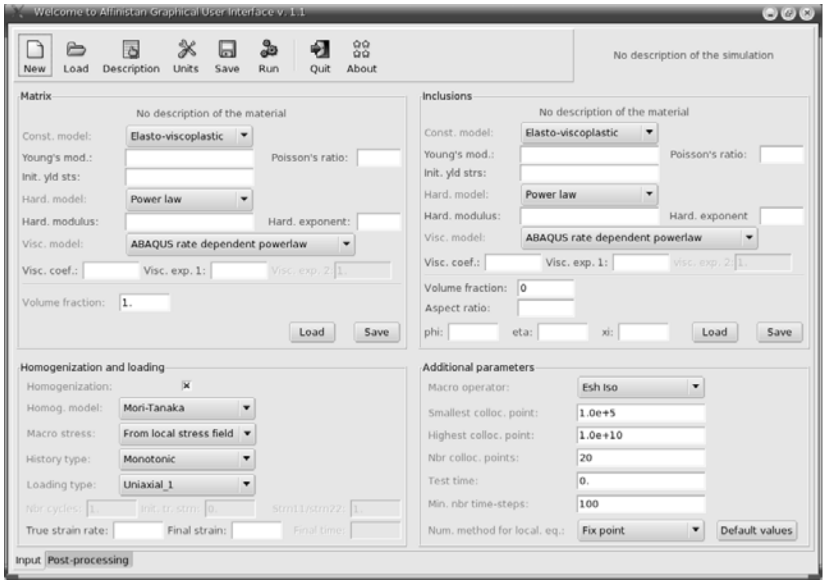

Figure F.1: Input section of Affinistan.

- Description: Give a description of both materials and of the simulation. These fields appear in the input window of the graphical user interface and in comments of the .dat file.
- Units: Define the global unit system (for stress, time and angles). A modification induces an optional automatic correction of the already filled fields.
- Save: Write the corresponding .dat file of the current simulation.
- Run: Run a simulation. If not done previously, the user is prompted to save the simulation. Some checks are made if the fields are filled correctly (each field label correctly filled is green if correct or red otherwise).
- Quit: Exit Affinistan.
- About: Give informations about the software.

F.1.2 Matrix and inclusions sections

- Const. model: Select the constitutive model: linear elastic, elasto-plastic or elasto-viscoplastic. For linear elastic materials, the initial yield stress is set very high and for elasto-plastic ones, the viscosity is set very low.

- Young's mod.: Young's modulus (E).
- Poisson's ratio: Poisson's ratio (ν).
- Init. yld strs: Initial yield stress (σ_Y).
- Hard. model: Hardening model: power law, exponential law or Swift law. The two first models are presented in section 6.1.
- Hard. modulus: Hardening modulus (k).
- Hard. exponent: Hardening exponent (n).
- Visc. model: Model for the viscoplastic function (g_v): Norton (see Doghri [24]), three-parameters creep model of ABAQUS [1], the viscous model defined by Li and Weng ([58]) or the ABAQUS rate-dependent power law [1]. Some of these models are presented in section 6.1.
- Visc. coef.: Viscoplastic coefficient.
- Visc. exp. 1: First viscoplastic exponent.
- Visc. exp. 2: Second viscoplastic exponent.
- Volume fraction: Volume fraction of each phase. If modified, volume fraction of the other phase is corrected accordingly.
- Aspect ratio: Aspect ratio of the spheroidal inclusions.
- Phi, eta and xi: Euler angles to describe the orientation of the inclusions with respect to the direction of traction. If aligned, all angles are nil.
- Load: Load a material properties file (.mat).
- Save: Save a material properties file (.mat).

F.1.3 Homogenization and loading section

- Homogenization: If checked, allows to define a heterogeneous material. Otherwise, only simulations on the matrix can be performed.
- Homog. model: Select the homogenization model: Voigt, Reuss, Mori-Tanaka, three-phases generalized self consistent (for spherical inclusions only) and interpolative model.
- Macro stress: Computation of the macroscopic stress response: average from local stress fields or from a linearized macroscopic constitutive law (suspended in the last version of Affinistan).

- History type: Monotonic, cyclic, relaxation or creep loading.
- Loading type: Prescribed strain, uniaxial traction along direction 1, biaxial traction along directions 1 and 2 or shear test in the plane 1/2.
- Nbr cycles: Specify the number of cycles if the loading history is cyclic.
- Init. tr. strain: Initial true strain if loading history is relaxation. Initial true stress if loading history is creep.
- Strn11/strn22: Strain ratio between directions 1 and 2 if loading type is biaxial.
- True strain rate: Constant true strain rate during all the simulation.
- Final strain.
- Final time: Computed from the two previous values.

F.1.4 Additional parameters section

- Macro operator: Select the way to compute the macroscopic operator (see section 5.3): only Eshelby's tensor is computed from an isotropic extraction of the affine modulus of the matrix or only the Hill's tensor P or all the computations.
- Smallest colloc. point: Smallest collocation point. Used in the numerical inversion of the Laplace-Carson transform.
- Highest colloc. point: Highest collocation point.
- Nbr colloc. points: Number of collocation points. These are equispaced on a logarithmic scale between the smallest and highest value.
- Test time: Reference time at which debugging information is written in several files. Inactive if nil.
- Min. nbr time-steps: Minimum number of time steps during the simulation.
- Num. method for local. eq.: Numerical method to solve the localization method: fixed point or Newton-Raphson.
- Default values: Reset all the fields of this section to their default values.

F.2 Post processing section

This section is used to plot or save figures. In addition to a new toolbar, it enables to add curves to the curves list (figure F.2) and to set some parameters for the layout of the figure (figure F.3).

F.2.1 Toolbar

- New figure: Delete all the curves from the curve list.
- View figure: Plot the curves list and the specified parameters for the layout. This figure is shown with the Gnuplot software for several seconds.
- Save figure: Save the current figure in a postscript format.
- Save script: Save the Gnuplot script corresponding to the current figure.
- Quit: Exit Affinistan.
- About: Give informations about the software.

F.2.2 Add curve section

A maximum of 20 curves can be plotted on the same figure.

- Select data source: Add a curve either from the last simulation or from a selected data file. If 'From simulation' is selected, the type of curve must be selected (macroscopic, in the matrix, in the inclusions, matrix alone or inclusions alone). Corresponding variables to be plotted must also be selected. If 'From file' option is selected the user is prompted to select the corresponding file and the column numbers of this file to be plotted.
- Curve label: Give a label to the current curve.
- Select line style: Select the line style. This option is only valid when saving the script.
- Select point style: Select the point style. This option is only valid when saving the script.

F.2.3 Set figure layout section

Enable to fix the layout of the figure. All these fields are optional.

- Figure title: Give a title to the figure.
- X Axis label: Give a label to the X axis.

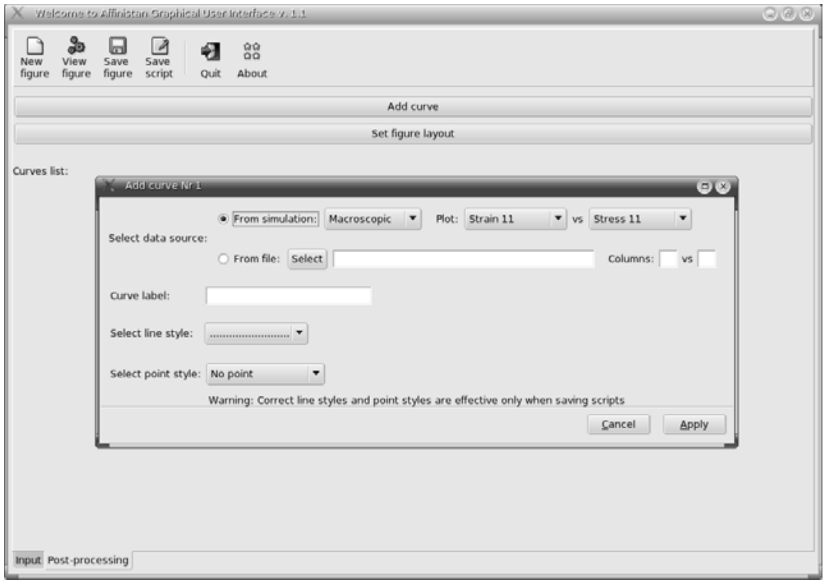

Figure F.2: Add curve section of Affinistan.

- Y Axis label: Give a label to the Y axis.
- X range: Define a range for the X axis.
- Y range: Define a range for the Y axis.
- Legend position: Select a corner of the figure for the legend position.

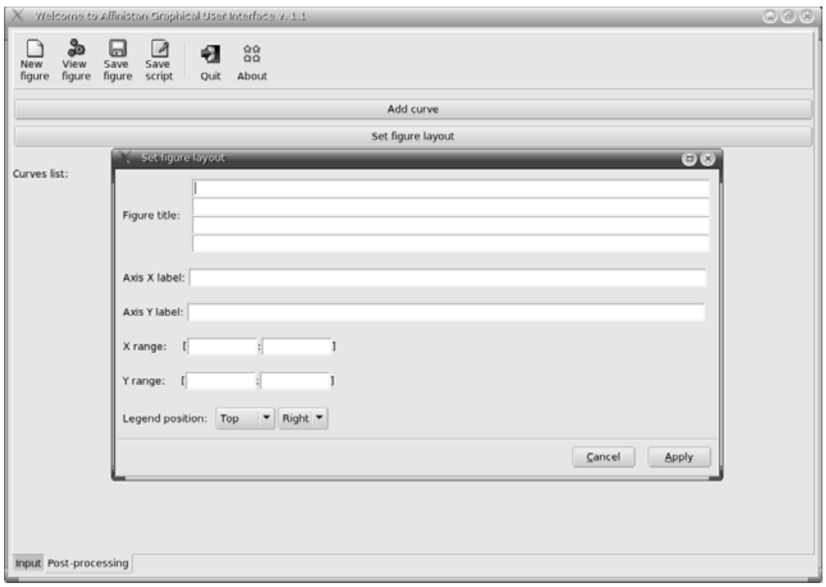

Figure F.3: Set figure layout section of Affinistan.

Appendix G

Notations and units

Fourth order tensors

Symbol	Definition	Units
$\boldsymbol{m}$	$\frac{\partial \dot{\boldsymbol{\varepsilon}}^{in}}{\partial \boldsymbol{\sigma}}$	$\frac{1}{s.Pa}$
$\boldsymbol{A}^{\epsilon}$	Strain concentration tensor ($\boldsymbol{\varepsilon}_1 = \boldsymbol{A}^{\epsilon} : \bar{\boldsymbol{\varepsilon}}$)	-
$\boldsymbol{B}^{\epsilon}$	Strain concentration tensor ($\boldsymbol{\varepsilon}_1 = \boldsymbol{A}^{\epsilon} : \boldsymbol{\varepsilon}_0$)	-
$\boldsymbol{C}$	Elastic or tangent operator	Pa
$\boldsymbol{C}^{*}$	Hill's constraint tensor	Pa
$\boldsymbol{C}^{alg}$	Algorithmic tangent operator	Pa
$\boldsymbol{C}^{ep}$	Continuum tangent operator (el.-pl.)	Pa
$\boldsymbol{C}^{in}$	Continuum tangent operator (el.-visc.pl.)	Pa
$\boldsymbol{C}^{s}$	Secant stiffness operator	Pa
$\boldsymbol{D}^{\varepsilon}$	Strain concentration tensor ($\boldsymbol{\varepsilon}(x) = \boldsymbol{D}^{\varepsilon} : \bar{\boldsymbol{\varepsilon}}$)	-
$\boldsymbol{D}^{\sigma}$	Stress concentration tensor ($\boldsymbol{\sigma}(x) = \boldsymbol{D}^{\sigma} : \bar{\boldsymbol{\sigma}}$)	-
$\boldsymbol{G}$	Relaxation tensor	Pa
$\boldsymbol{I}^{vol}$	Volumetric unit tensor	-
$\boldsymbol{I}^{dev}$	Deviatoric unit tensor	-
$\boldsymbol{I}$	Unit tensor	-
$\boldsymbol{J}$	Creep tensor	$1/Pa$
$\boldsymbol{P}$	Hill's tensor	$1/Pa$
$\boldsymbol{S}$	Compliance	$1/Pa$
$\mathcal{E}$	Eshelby's tensor	-

Second order tensors

Symbol	Definition	Units
$\boldsymbol{l}$	$\frac{\partial g_v}{\partial \boldsymbol{\sigma}}$	$\frac{1}{s.Pa}$
$\boldsymbol{n}$	$\frac{\partial \dot{\boldsymbol{\varepsilon}}^{in}}{\partial p}$	$1/s$
$\boldsymbol{G}$	Displacement gradient	-
$\boldsymbol{N}$	Normal to the yield surface in stress space	-
$\boldsymbol{\alpha}$	Thermal expansion	1/K
$\mathbf{1}$	Unit tensor	-
$\boldsymbol{\varepsilon}$	Strain	-
$\boldsymbol{\varepsilon}^e$	Elastic strain	-
$\boldsymbol{\varepsilon}^p$	Plastic strain	-
$\boldsymbol{\varepsilon}^{th}$	Thermal strain	-
$\boldsymbol{\varepsilon}^*$	Eigenstrain	-
$\boldsymbol{\varepsilon}^\infty$	Far field strain	-
$\boldsymbol{\sigma}$	Stress	Pa
τ	Polarization tensor	Pa

Scalars

Symbol	Definition	Units
f	Yield function	Pa
g_v	Viscoplastic function	$1/s$
p	Accumulated plastic strain	-
q	$\frac{\partial g_v}{\partial p}$	$1/s$
v_1	Volume fraction of inclusions	-
w	Stress potential	Pa
E	Young's modulus	Pa
G	Lamé Coefficient	Pa
$R(p)$	Hardening function	Pa
S	Surface	m^2
T	Temperature	K
V	Volume	m^3
$\dot{\gamma}$	Plastic multiplier	-
κ	Bulk modulus	Pa
λ	Lamé coefficient	Pa
μ	Shear modulus	Pa
ν	Poisson's ratio	-
σ_{eq}	Equivalent stress	Pa
σ_{eq}^{tr}	Trial equivalent stress after an elastic time step	Pa
σ_Y	Initial yield stress	Pa

Vectors

Symbol	Definition	Units
$\boldsymbol{n}$	Normal to a surface	-
$\boldsymbol{t}$	Stress	Pa
$\boldsymbol{u}$	Displacement	m
$\boldsymbol{x}$	Position	m

Symbols

Symbol	Definition
$\tilde{x}_r$	Reference state in phase r
$< x >_{\omega_r}$	Average value over phase r
$< x >_{\omega}$	Average value over all the volume
$\bar{x}$	Macroscopic value
$\boldsymbol{C} > \boldsymbol{0}$	$\boldsymbol{\varepsilon} : \boldsymbol{C} : \boldsymbol{\varepsilon} > 0$ for all $\boldsymbol{\varepsilon}$
Δx	Variation
$\otimes$	Convolution product
$\odot$	Stieljes-type convolution product
x^*	Laplace-Carson transform
$[\mathcal{L}(x)]_{(s)}$	Laplace-Carson transform of an expression
s	Laplace variable
x_0	Refers to the matrix
x_1	Refers to the inclusions
$\boldsymbol{x}^{dev}$	Deviatoric part of the tensor
x^{eff}	Effective value
$\dot{x}$	Time derivative
$\otimes$	Tensorial product
$:$	Contraction over two indices
$::$	Contraction over four indices

Bibliography

[1] ABAQUS®. *A general-purpose finite element software.* ABAQUS Inc., Pawtucket, RI, USA, 2005.

[2] Aboudi, J. Micromechanical analysis of composites by the method of cells. *Appl. Mech. Rev. 42* (1989), 193–221.

[3] Aboudi, J., Pindera, M.-J., and Arnold, S. Linear thermo-elastic higher-order theory for periodic multiphase materials. *J. Appl. Mechanics 68* (2001), 697–707.

[4] Aboudi, J., Pindera, M.-J., and Arnold, S. Higher-order theory for periodic multiphase materials with inelastic phases. *Int. J. Plasticity 19*, 6 (2003), 805–847.

[5] Bednarcyk, B., Arnold, S., Aboudi, J., and Pindera, M.-J. Local field effects in titanium matrix composites subject to fiber-matrix debonding. *Int. J. Plasticity 20* (2004), 1707–1737.

[6] Bensoussan, A., Lions, J., and Papanicolaou, G. *Asymptotic analysis for periodic structures.* North Holland, Amsterdam, 1978.

[7] Benveniste, Y. A new approach to the application of Mori-Tanaka's theory in composite materials. *Mech. Materials 6*, 2 (1987), 147–157.

[8] Berveiller, M., and Zaoui, A. An extension of the self-consistent scheme to plastically-flowing polycrystals. *J. Mech. Phys. Solids 26* (1979), 325–344.

[9] Böhm, H., and Han, W. Comparisons between three-dimensional and two-dimensional multi-particle unit cell models for particle reinforced metal matrix composites. *Modeling and Simulation in Materials Science and Engineering 2* (2001), 47–65.

[10] Bornert, M. *Morphologie microstructurale et comportement mécanique; caractérisations expérimentales, approches par bornes et estimations autocohérentes généralisées.* Phd thesis, Ecole Nationale des Ponts et Chaussées, 1996.

[11] Bornert, M. *Homogénéisation des milieux aléatoires: bornes et estimations*, vol. 1. Hermes Science, Paris, 2001, ch. 5, pp. 133–221.

[12] Bornert, M., Stoltz, C., and Zaoui, A. A morphologically representative pattern-based bounding in elasticity. *J. Mech. Phys. Solids 44* (1996), 307–331.

[13] Bowles, D., and Tompkins, S. Prediction of coefficients of thermal expansion for unidirectional composites. *J. Comp. Mat. 23* (1989), 370–388.

[14] Brenner, R., Castelnau, O., and Badea, L. Mechanical field fluctuations in polycrystals estimated by homogenization techniques. *Proc. Roy. Soc. Lond. A 460* (2004), 3589–3612.

[15] Brenner, R., Masson, R., Castelnau, O., and Zaoui, A. A "quasi-elastic" affine formulation for the homogenised behaviour of nonlinear viscoelastic polycrystals and composites. *Eur. J. Mech. A/Solids 25* (2002), 943–960.

[16] Budianski, B., and Wu. Theoretical prediction of plastic strains of polycrystals. In *Proc. of the 4th U.S. National Congress of Applied Mechanics, ASME* (1962), pp. 1175–1185.

[17] Buryachenko, V. The overall elastoplastic behavior of multiphase materials with isotropic components. *Acta Mech. 119* (1996), 93–117.

[18] Chaboche, J., and Kanouté, P. Sur les aproximations 'isotrope' et 'anisotrope' de l'opérateur tangent pour les méthodes tangentes, incrémentale et affine. *C. R. Acad. Sci. Paris* (2003), 857–864.

[19] Chaboche, J., Kanouté, P., and Roos, A. On the capabilities of mean-field approaches for the description of plasticity in metal matrix composites. *Int. J. Plasticity 21*, 7 (2005), 1409–1434.

[20] Christman, T., Needleman, A., and Suresh, S. An experimental and numerical study of deformation in metal-ceramic composites. *Acta Metall. 37*, 11 (1989), 3029–3050.

[21] Chung, P., Tamma, K., and Namburu, R. Asymptotic expansion homogenization for heterogeneous media: computational issues and applications. *Composite part A 32*, 9 (2001), 1291–1301.

[22] deBotton, G., and Ponte Castañeda, P. Variational estimates for the creep behavior of polycrystals. *Proc. Roy. Soc. Lond. A 448* (1995), 421–442.

[23] DIGIMAT. *A software for the linear and nonlinear multi-scale modeling of heterogeneous materials*. e-Xstream engineering, Louvain-la-Neuve, Belgium, 2006.

[24] Doghri, I. *Mechanics of deformable solids. Linear, nonlinear, analytical and computational aspects*. Springer, Berlin, 2000.

[25] Doghri, I., and Friebel, C. Effective elasto-plastic properties of inclusion-reinforced composites. Study of shape, orientation and cyclic response. *Mech. Materials 37*, 1 (2005), 45–68.

[26] Doghri, I., and Ouaar, A. Homogenization of two-phase elasto-plastic composite materials and structures. Study of tangent operators, cyclic plasticity and numerical algorithms. *Int. J. Solids Struct. 40*, 7 (2003), 1681–1712.

[27] Doghri, I., and Tinel, T. Micromechanical modeling and computation of elasto-plastic materials reinforced with distributed-orientation fibers. *Int. J. Plasticity 21*, 10 (2005), 1919–1940.

[28] Drugan, W., and Willis, J. A micromechanics-based nonlocal constitutive equations and estimates of representative volume element size for elastic composites. *J. Mech. Phys. Solids 44* (1996), 497–524.

[29] Dvorak, G. Transformation field analysis of inelastic composite materials. *Proc. Roy. Soc. Lond. A 437* (1992), 311–327.

[30] Eshelby, J. The determination of the elastic field of an ellipsoidal inclusion, and related problems. *Proc. Roy. Soc. Lond. A 241* (1957), 376–396.

[31] Frederico, S., Grillo, A., and Herzog, W. A transversely isotropic composite with a statistical distribution of spheroidal inclusions: a geometrical approach to overall properties. *J. Mech. Phys. Solids 52*, 10 (2004), 2309–2327.

[32] Friebel, C. *Modélisation et Simulation micro-macro de matériaux composites. Etude de l'influence des renforts (matériau, forme et orientation)*. Graduation report, Université Catholique de Louvain, Belgium, 2002.

[33] Friebel, C., Doghri, I., and Legat, V. General mean-field homogenization schemes for viscoelastic composites containing multiple phases of coated inclusions. *Int. J. Solids Struct. 43*, 9 (2006), 2513–2541.

[34] Gavazzi, A., and Lagoudas, D. On the numerical evaluation of eshelby's tensor and its application to elastoplastic fibrous composites. *Comp. Mech. 7* (1990), 13–19.

[35] Ghosh, S., Lee, K., and Moorthy, S. Multiple scale analysis of heterogeneous elastic structures using homogenization theory and Voronoi cell finite element method. *Int. J. Solids Struct. 32*, 1 (1995), 27–62.

[36] Ghosh, S., Lee, K., and Moorthy, S. Two scale analysis of heterogeneous elastic-plastic materials with asymptotic homogenization and Voronoi cell finite element model. *Comput. Methods Appl. Mech. Engrg. 132*, 1-2 (1996), 63–116.

[37] González, C., Segurado, J., and LLorca, J. Numerical simulation of elasto-plastic deformation of composites: evolution of stress microfields and implications for homogenization models. *J. Mech. Phys. Solids 52*, 7 (2004), 1573–1593.

[38] Hashin, Z., and Shtrikman, S. A variational approach to the theory of the elastic behaviour of multiphase materials. *J. Mech. Phys. Solids 11* (1963), 127–140.

[39] Hervé, E., and Zaoui, A. n-layered inclusion-based micromechanical modelling. *Int. J. Engrg. Sci. 31* (1993), 1–10.

[40] Hervé, E., and Zaoui, A. Elastic behavior of multiply coated fiber-reinforced composites. *Int. J. Engrg. Sci. 33* (1995), 1419–1433.

[41] Hill, R. Elastic properties of reinforced solids: some theoretical principles. *J. Mech. Phys. Solids 11* (1963), 357–372.

[42] Hill, R. Continuum micro-mechanics of elastoplastic polycrystals. *J. Mech. Phys. Solids 13*, 2 (1965), 89–101.

[43] Hill, R. A self-consistent mechanics of composite materials. *J. Mech. Phys. Solids 13*, 4 (1965), 213–222.

[44] Hom, C. Three-dimensional finite element analysis of plastic deformation in a whisker-reinforced metal matrix composite. *J. Mech. Phys. Solids 40*, 5 (1992), 991–1008.

[45] Jansson, S. Homogenized nonlinear constitutive properties and local stress concentration for composites with periodic internal structure. *Int. J. Solids Struct. 29*, 17 (1992), 2181–2200.

[46] Jiang, M., Jasiuk, I., and Ostoja-Starzewski, M. Apparent elastic and elastoplastic behavior of periodic composites. *Int. J. Solids Struct. 39* (2002), 199–212.

[47] Jiang, M., Ostoja-Starzewski, M., and Jasiuk, I. Scale-dependent bounds on effective elastoplastic response of random composites. *J. Mech. Phys. Solids 49* (2001), 655–673.

[48] Ju, J. Consistent tangent moduli for a class of viscoplasticity. *J. Engrg. Mech.-ASCE 116*, 8 (1990), 1764–1779.

[49] Kang, G.-Z., and Gao, Q. Tensile properties of randomly oriented short $\delta - al_2o_3$ fiber reinforced aluminum alloy composites: II. Finite element analysis for stress transfer, elastic modulus and stress-strain curve. *Composite part A 33*, 5 (2002), 657–667.

[50] Kanit, T., Forest, S., Galliet, I., Mounoury, V., and Jeulin, D. Determination of the size of the representative volume element for random composites: statistical and numerical approach. *Int. J. Solids Struct. 40*, 13-14 (2003), 3647–3679.

[51] Kouznetsova, V. Computational homogenization. Micromechanics graduate course lecture notes, Eindhoven, November 2004.

[52] Kouznetsova, V., Geers, M., and Brekelmans, W. Multi-scale constitutive modelling of heterogeneous materials with a gradient-enhanced computational homogenization scheme. *Int. J. Num. Meth. Engrg. 54* (2002), 1235–1260.

[53] Kouznetsova, V., Geers, M., and Brekelmans, W. Multi-scale second-order computational homogenization of multi-phase materials: a nested finite element solution strategy. *Comput. Methods Appl. Mech. Engrg. 193* (2004), 5525–5550.

[54] Kröner, E. Zur plastischen verformung des vielkristalls. *Acta Metall. 9*, 2 (1961), 155–161.

[55] Levin, V. Thermal expansion coefficients of heterogeneous materials. *Mekh. Tverd. Tela 8* (1967), 38–94.

[56] Levy, A., and Papazian, J. Tensile properties of short fiber-reinforced SiC/Al composites: Part II. Finite element analysis. *Metall. Trans. A 21*, 2 (1990), 411–420.

[57] Li, G., and Ponte Castañeda, P. *Variational estimates for the elasto-plastic response of particle-reinforced metal-matrix composites*, vol. 47. American Society of Mechanical Engineers, 1994, pp. S77–S94.

[58] Li, J., and Weng, G. A secant viscosity approach to the time-dependent creep of an elasto-viscoplastic composite. *J. Mech. Phys. Solids 45*, 7 (1997), 1069–1083.

[59] Li, J., and Weng, G. A unified approach from elasticity to viscoelasticity to viscoplasticity of particle-reinforced solids. *Int. J. Plasticity 14*, 1-3 (1998), 193–208.

[60] Li, J., and Weng, G. Creep of a composite with dual viscoplastic phases. *Compos. Science and Technology 58*, 11 (1999), 1803–1810.

[61] Lielens, G. *Micro-Macro Modeling of Structured Materials.* Phd thesis, Université Catholique de Louvain, Belgium, 1999.

[62] Lielens, G., Pirotte, P., Couniot, A., Dupret, F., and Keunings, R. Prediction of thermo-mechanical properties for compression moulded composites. *Composite part A 29*, 1-2 (1998), 63–70.

[63] Lin, A., and Han, S.-P. On the distance between two ellipsoids. *SIAM J. Opt. 13*, 1 (2002), 298–308.

[64] LLorca, J., and Segurado, J. Three-dimensional multiparticle cell simulations of deformation and damage in sphere-reinforced composites. *Mater. Sci. Eng. A 365*, 1-2 (2004), 267–274.

[65] Lusti, H., Hine, P., and Gusev, A. Direct numerical predictions for the elastic and thermoelastic properties of short fiber composites. *Compos. Science and Technology 62* (2002), 1927–1934.

[66] Masson, R. *Estimations non linéaires du comportement global de matériaux hétérogènes en formulation affine.* Phd thesis, Ecole Polytechnique, Paris, France, 1998.

[67] Masson, R., Bornert, M., Suquet, P., and Zaoui, A. An affine formulation for the prediction of the effective properties of nonlinear composites and polycrystals. *J. Mech. Phys. Solids 48*, 6-7 (2000), 1203–1227.

[68] Masson, R., and Zaoui, A. Self-consistent estimates for the rate-dependent elasto-plastic behavior of polycrystalline materials. *J. Mech. Phys. Solids 47*, 7 (1999), 1543–1568.

[69] Molinari, A., Canova, G., and Ahzi, S. A self consistent approach at the large deformation polycrystal viscoplasticity. *Acta Metall. 35*, 12 (1987), 2983–2994.

[70] Moulinec, H., and Suquet, P. A fast numerical method for computing the linear and nonlinear properties of composites. *C. R. Acad. Sci. Paris II 318* (1994), 1417–1423.

[71] Moulinec, H., and Suquet, P. *A FFT-based numerical method for computing the mechanical properties of composites from images of their microstructure.* Kluwer Academic Publ., Dordrecht, 1995, pp. 235–246.

[72] NETGEN. *An automatic three-dimensional tetrahedral mesh generator.* Joachim Schöberl, Johannes Kepler University, Linz, Austria, 2004.

[73] Ostoja-Starzewski, M. Material spatial randomness: From statistical to representative volume element. *Prob. Eng. Mech. 21* (2006), 112–132.

[74] Paley, M., and Aboudi, J. Micromechanical analysis of composites by the generalized cells model. *Mech. Materials 14*, 2 (1992), 127–139.

[75] Palmyra. *A finite-element software for heterogeneous micro-structures.* MatSim GmbH, Zurich, Switzerland, 2001.

[76] Pan, Y., and Chou, T. Point force solution for an infinite transversely isotropic solid. *J. Appl. Mechanics 43*, 4 (1976), 608–612.

[77] Pierard, O. *Micro/macro study of reinforced polymers and polymeric composites. Mathematical modeling and numerical simulation of elasto-viscoplastic behavior and thermal coupling.* DEA graduation report, Université Catholique de Louvain, Belgium, 2004.

[78] Pierard, O., and Doghri, I. An enhanced affine formulation and the corresponding numerical algorithms for the mean-field homogenization of elasto-viscoplastic composites. *Int. J. Plasticity 22*, 1 (2006), 131–157.

[79] Pierard, O., and Doghri, I. A study of various estimates of the macroscopic tangent operator in the incremental homogenization of elasto-plastic composites. *Int. J. Mult. Comp. Engrg.* (2006). Accepted for publication.

[80] Pierard, O., Friebel, C., and Doghri, I. Mean-field homogenization of multi-phase thermo-elastic composites: a general framework and its validation. *Compos. Science and Technology 64*, 10-11 (2004), 1587–1603.

[81] Pierard, O., González, C., Segurado, J., LLorca, J., and Doghri, I. Micromechanics of elasto-plastic materials reinforced with ellipsoidal inclusions. *Mech. Materials* (2006). Submitted for publication.

[82] Pierard, O., LLorca, J., Segurado, J., and Doghri, I. Micromechanics of particle-reinforced elasto-viscoplastic composites: finite element simulations versus affine homogenization. *Int. J. Plasticity* (2006). Submitted for publication.

[83] Ponte Castañeda, P. The effective mechanical properties of nonlinear isotropic composites. *J. Mech. Phys. Solids 39* (1991), 45–71.

[84] Ponte Castañeda, P. Exact second-order estimates for the effective mechanical properties of nonlinear composite materials. *J. Mech. Phys. Solids 44*, 6 (1996), 827–862.

[85] Ponte Castañeda, P. Second-order homogenization estimates for nonlinear composites incorporating field fluctuations: I-theory. *J. Mech. Phys. Solids 50*, 4 (2002), 737–757.

[86] Ponte Castañeda, P. Variational methods in nonlinear homogenization. In *Approche multi-échelles en mécanique des matériaux* (Aussois, 2006), MECAMAT.

[87] Ponte Castañeda, P., and Willis, J. The effect of spatial distribution on the effective behavior of the composite materials and cracked media. *J. Mech. Phys. Solids 43* (1995), 1919–1951.

[88] Povirk, G. Incorporation of microstructural information into models of two-phase materials. *Acta Metall. Mater. 43*, 8 (1995), 3199–3206.

[89] Sanchez-Palencia, E. *Non homogeneous media and vibration theory - lecture notes in physics 127.* Springer, Berlin, 1980.

[90] Schapery, R. Approximate methods of transform inversion in viscoelastic stress analysis. In *Proceedings of the 4th US National Congress on Applied Mechanics* (1962), vol. 2, pp. 1075–1085.

[91] Scholes, J. Solution of the problem b6 of the 1st putnam, 1938. http://www.kalva.demon.co.uk/putnam/psoln/psol3813.html, 2002.

[92] Segurado, J., and LLorca, J. A numerical approximation to the elastic properties of sphere-reinforced composites. *J. Mech. Phys. Solids 50*, 10 (2002), 2107–2121.

[93] Segurado, J., and LLorca, J. A computational micromechanics study of the effect of interface decohesion on the mechanical behavior of composites. *Acta Mater. 53* (2005), 4931–4942.

[94] Suquet, P. Overall properties of nonlinear isotropic composites. *C. R. Acad. Sci. Paris IIb 320* (1995), 563–571.

[95] Suquet, P. *Effective properties of nonlinear composites*, vol. 377. Springer-Verlag, Udine, Italy, 1997, pp. 197–264.

[96] Suquet, P., and Bornert, M. *Rappels de calcul tensoriel et d'élasticité*, vol. 2. Hermes Science, Paris, 2001, ch. 5, pp. 171–202.

[97] Suquet, P., and Ponte Castañeda, P. Small-contrast perturbation expansions for the effective properties of nonlinear composites. *C. R. Acad. Sci. Paris II 317* (1993), 1515–1522.

[98] Takao, Y., and Taya, M. The effect of variable fiber aspect ratio on the stiffness and thermal expansion coefficients of a short fiber composite. *J. Comp. Mat. 21* (1987), 140–156.

[99] Torquato, S. Morphology and effective properties of disordered heterogeneous media. *Int. J. Solids Struct. 35* (1998), 2385–2406.

[100] Tucker, C., and Liang, E. Stiffness predictions for unidirectional short-fiber composites: Review and evaluation. *Compos. Science and Technology 59* (1999), 655–671.

[101] van Es, M. *Polymer-clay Nanocomposites. The importance of particle dimensions.* PhD thesis, Technische Universiteit Delft, The Netherlands, 2001.

[102] Walpole, L. On bounds for the overall elastic moduli of inhomogeneous systems -I. *J. Mech. Phys. Solids 14* (1966), 151–162.

[103] Walpole, L. Elastic behavior of composite materials: theoretical foundations. *Adv. in Appl. Mech. 21* (1981), 169–242.

[104] Weissenbek, E., Böhm, H., and Rammerstorfer, F. Micromechanical investigations of arrangement effects in particle reinforced metal matrix composites. *Comput. Mat. Science 3* (1994), 263–278.

[105] Weng, G. The theoretical connection between Mori-Tanaka and the Hashin-Shtrikman-Walpole bounds. *Int. J. Engrg. Sci. 28* (1990), 1111–1120.

[106] Widom, B. Random sequential adsortion of hard spheres to a volume. *J. Chem. Phys. 44* (1966), 3884–3894.

[107] Willis, J. Bounds and self-consistent estimates for the overall moduli of anisotropic composites. *J. Mech. Phys. Solids 28* (1977), 185–202.

[108] Withers, P. The determination of the elastic field of an ellipsoidal inclusion in a transversely isotropic medium and its relevance to composite materials. *Philosophical Magazine A 59*, 4 (1989), 759–781.

[109] Yi, Y.-M., Park, S.-H., and Youn, S.-K. Asymptotic homogenization of viscoelastic composites with periodic microstructures. *Int. J. Solids Struct. 35*, 17 (1996), 2039–2055.

[110] Zaoui, A. Continuum micromechanics: Survey. *J. Engrg. Mech.-ASCE 128*, 8 (2002), 808–816.